Fossil Record 25 (2) 2022, 231–261 | DOI 10.3897/fr.25.85621

PENSOFT

für Natur MUSEUM FÜR NATURKUNDE BERLIN

The outstanding suction-feeder *Marcopoloichthys furreri* new species (Actinopterygii) from the Middle Triassic Tethys Realm of Europe and its implications for early evolution of neopterygian fishes

Gloria Arratia[1,2]

1 *Biodiversity Institute, University of Kansas, Dyche Hall, 1345 Jayhawk Blvd., Lawrence, Kansas 66045, USA*

2 *Department of Ecology and Evolutionary Biology, University of Kansas, Lawrence, Kansas 66045, USA*

https://zoobank.org/48170AC2-9C0B-42AF-9CCD-3C770113F4CE

Corresponding author: Gloria Arratia (garratia@ku.edu)

Academic editor: Florian Witzmann ♦ **Received** 20 April 2022 ♦ **Accepted** 14 June 2022 ♦ **Published** 5 July 2022

Abstract

Marcopoloichthys furreri **sp. nov.**, a small scaleless fish from the Ladinian of Switzerland, is described based on ten well preserved specimens, which provide outstanding morphological information, allowing the re-study of the family and generic diagnoses that were solely based on a few Eurasian marcopoloichthyids. An exhaustive investigation of morphological features of *M. furreri* provides evidence of new morphological structures not previously known in Triassic neopterygians (e.g., supraneural carrier; two pairs of nasal bones; mesethmoid; series of three bony postcleithra) that are interpreted as autapomorphies of *Marcopoloichthys*, which occur together with some primitive features (e.g., lack of supramaxillae; presence of surangular and coronoid; aspondylous vertebral column; clavicle present). The combination of primitive and advanced characters proved to be critical when *M. furreri* was added to a previous hypothesis of neopterygian relationships, because it provided unquestionable support for *Marcopoloichthys* as a stem teleost or teleosteomorph. Some characters supporting this interpretation are the presence of a mobile premaxilla; an unpaired vomer; and first and last principal rays forming leading margins of caudal fin. Additionally, *Marcopoloichthys furreri*, due to a combination of teleostean synapomorphies (e.g., epineural processes; four pectoral radials; propterygium fused with first pectoral ray), stands in a polytomy with aspidorhynchiforms and more advanced teleosteomorphs in another phylogenetic analysis. Consequently, the combination of characters of *Marcopoloichthys* is relevant for understanding the taxonomy and systematics of crown neopterygians. Marcopoloichthyids were suction-feeding fishes, and the excellent preservation of the new species permits discussion of the anatomical modifications involved in the feeding and resting processes.

Key Words

advanced Neopterygii, Ladinian, morphology, Prosanto Formation, Switzerland, systematics, taxonomy

Introduction

The new material studied here was recovered in Ducanfurgga in a few localities of the Prosanto Formation near Davos, Canton Graubünden (Grisons), Swiss Alps. The Prosanto Formation forms part of the marine Middle Triassic (Ladinian) from the Silvretta Nappe (Fig. 1). The depositional environment of the Prosanto Formation is interpreted as a localized basin with a stratified waterbody that resulted in oxygen-depleted bottom water. Details of the geology, stratigraphy, and paleoecology have been described by Eichenberger (1986), Bürgin et al. (1991), Furrer et al. (1992), and Furrer (1995, 1999, 2004). After reviewing the lithology of the specimens, which is always a finely laminated grey limestone typical of the uppermost Prosanto Formation, it is suggested that all the specimens included in this contribution originated from this uppermost part, about 10 to 20 meters below the upper boundary and a few meters above the volcanic ash layer known as “Ducan I” (Furrer pers. com., December 2021).

Starting in 1989, a large number of new fossils from the Prosanto Formation had been discovered in systematic excavations by Dr. Heinz Furrer and his team from the University of Zurich. The recovered fossils include calcareous algae, bivalves, gastropods, cephalopods, crustaceans (Bürgin et al. 1991), and vertebrates, such as fishes and reptiles, with the fish fauna largely dominated by the actinopterygian *Habroichthys* (Bürgin 1999; Furrer 2019). The fishes that have been described are mainly actinopterygians, such as saurichthyiforms (e.g., *Saurichthys curionii* [Bellotti, 1857], *S. costasquamosus* Rieppel, 1985), perleidiforms (e.g., *Platysiagum minus* Egerton, 1872; *Ctenognathichthys bellotti* Bürgin, 1992; *Ctenognathichthys hattichi* Bürgin & Herzog, 2002; *Peltoperleidus ducanensis* Bürgin et al., 1991), peltopleuriforms (*Peltopleurus lissocephalus* Brough, 1939; *Peripeltopleurus vexillipinnis* Bürgin, 1992; *Peltoperleidus obristi* Herzog, 2001), stem neopterygians (*Habroichthys minimus* Brough, 1939 and Bürgin 1990; *H. griffithi* Bürgin, 1992), and parasemionotiforms (e.g., *Eoeugnathus megalepis* Brough, 1939 and Herzog 2003; and *Prosantichthys buergeni* Arratia & Herzog, 2007). Undescribed actinopterygians include *Colobodus* sp., *Luganoia* sp., *Eosemionotus* sp., *Archaeosemionotus* sp, and many others (see Bürgin 1999: appendix 2 and Furrer 2019), as well as two coelacanthiforms, *Ticinepomis peyeri* (Cavin et al., 2013) and *Foreyia maxkuhni* (Cavin et al., 2017).

Among the fishes mentioned in the literature, there are three specimens from the Prosanto Formation that

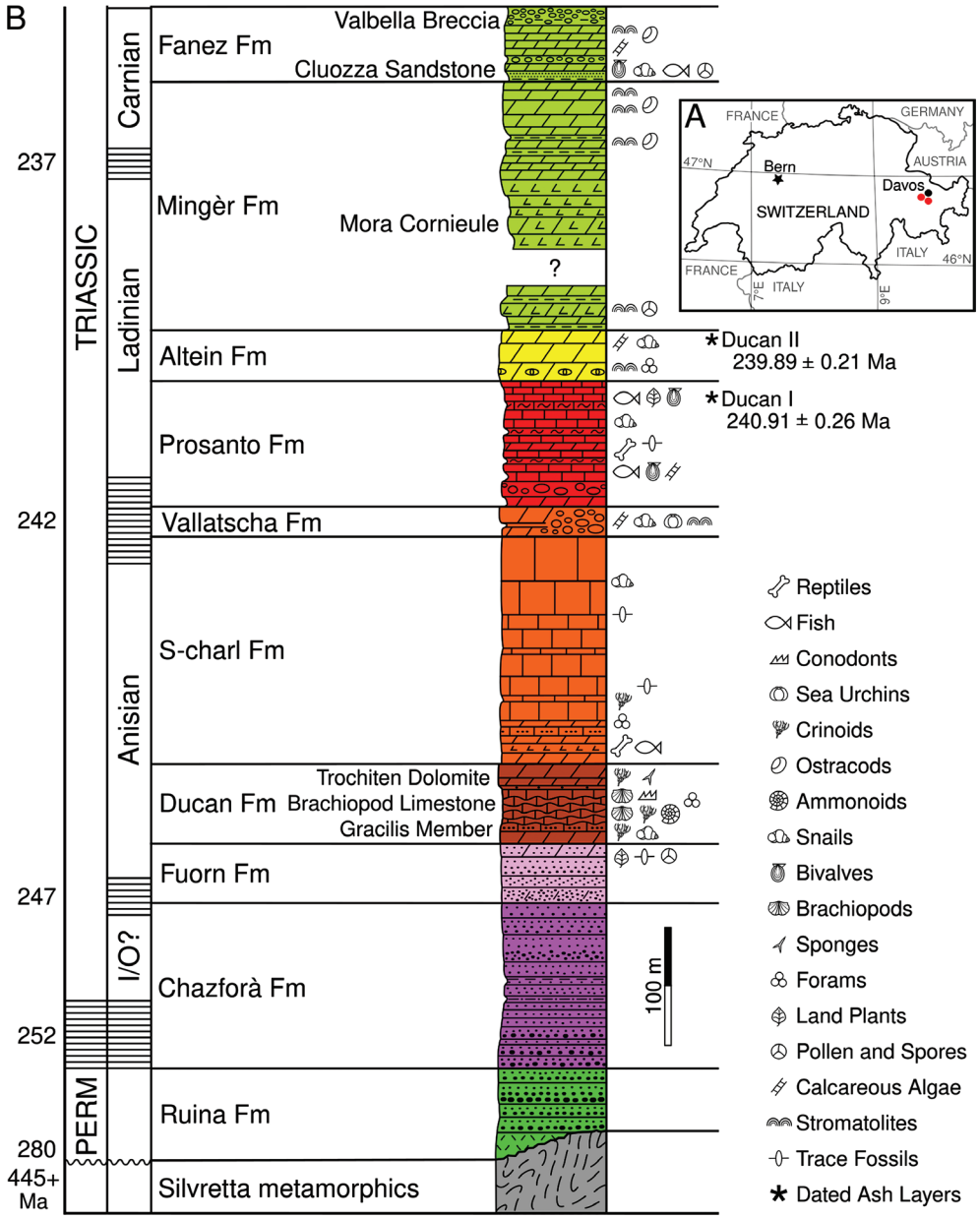

Figure 1. A. Approximate geographic position of localities containing *Marcopoloichthys furreri* sp. nov., indicated with red circles; **B.** Stratigraphy of the Silvreta Nappe with special emphasis of the Prosanto Formation and distribution of faunas and floras. Abbreviated and slightly modified from Furrer (2019: fig. 11).

were previously identified as *Prohalecites* sp. (Bürgin et al. 1991) or Neopterygii incertae sedis gen. et sp. indet. (Bürgin 1999: fig. 8) that are included in this study. These specimens, plus six others collected between 1991 and 2003 in the Early Ladinian strata of the Prosanto Fm., were preliminarily listed in the catalogue as "gen. and sp. indet.", which included a young individual about 23 mm maximum length. Due to their preservation, a long process of careful preparation was required, which revealed features common to all of them. In 2021, a new specimen of this fish was collected. These ten specimens are studied herein, including an extensive anatomical description allowed by the excellent preservation, plus the description of a few anatomical structures previously unreported in fish anatomy. They are assigned to the family Marcopoloichthyidae and its genus *Marcopoloichthys* (Tintori et al., 2007), whose original diagnoses are based on much lesser quality material from the Anisian of China (*Marcopoloichthys ani*) and the Norian of Italy (*M. ani*, *M. andreettii*, and *M. faccii*, which was previously described as *Pholidophorus faccii* by Gortani in 1907). Marcopoloichthyids were broadly interpreted as basal neopterygians by Tintori et al. (2017), following Patterson's (1973) conception of Neopterygii, although the authors mentioned certain similarities with the Middle Triassic teleosteomorph *Prohalecites*.

Marcopoloichthyids, which are small fishes of about 5 cm maximum length, are easy to identify because of their special mouth configuration as suction feeders together with a naked body and a vertebral column with a persistent, functional notochord and well-developed arcocentral vertebral elements. The nice preservation of the new species described herein from the Prosanto Formation in Switzerland allows the description of several cranial and vertebral column characters that were unknown, making this the most completely known species within the family. Additionally, specimens of different sizes exhibit ontogenetic changes that lead to reevaluation of the family and generic diagnoses, and the excellent preservation of specimens with closed and open mouths yields an understanding of the suction feeding mechanism of marcopoloichthyids. A phylogenetic analysis was conducted to investigate the position of these fishes among Neopterygii.

Material and methods

The material studied here consists of ten specimens, nine of which are catalogued in the collections of the Paleontological Institute and Museum, University of Zurich, Switzerland (**PIMUZ**) and one in the Bündner Naturmuseum, Chur, Canton Graubünden (**BNM**). Most of the specimens were found at localities in the so-called "Ducan" mountain chain: Ducanfurgga, Ducantal, Gletscher Ducan and the upper Val da Stugl—all within three km on both sides of the mountain "Gletscher Ducan" (Fig. 1; Table 1).

The older collected specimens used in the description of the new species were mechanically prepared by Angela Ceola and Christian Obrist, whereas the most recently collected were both mechanically prepared by Christin Obrist and acid prepared (3–5% formic acid) by Heinz Furrer.

Wild FM 8 and Leica MZ9 stereomicroscopes equipped with a camera lucida were used by the author to prepare the line drawings of the specimens. Parts of the specimens were photographed under normal light at the Museum für Naturkunde, Leibniz Institute for Evolution and Biodiversity Science (Berlin, Germany); others were photographed at the Paleontological Institute and Museum, University of Zurich. Most illustrations are based directly on specimens; a few are based on photographs. Photographs are not retouched with Photoshop. The latter was only used to label figures.

Anatomical terminology

The terminology of the skull roof bones follows Westoll (1943), Jollie (1962), and Schultze (2008 and literature cited therein) that has been recently confirmed using other evidence (Teng et al. 2019). To avoid confusion, the first time that the parietal and postparietal bones are cited in the text, as well as in all figures, the traditional terminology is shown in square brackets, e.g., parietal bone [= frontal]: pa [= fr]. The terminology of the vertebral column follows Arratia et al. (2001) and Arratia (2015), whereas that of the caudal endoskeletal elements and caudal skeletal types (e.g., polyural or diural) follows Nybelin (1963), Schultze and Arratia (1988, 1989, 2013), and Arratia and Schultze (1992, 2013). The count of vertebrae follows Tintori et al. (2007) to ensure that the results are comparable. The

Table 1. Record of specimens of *Marcopoloichthys furreri* sp. nov. from the Prosanto Formation (Early Ladinian), Switzerland.

Catalogue Nr.	Locality	Community	Date	References
A/I 1194	Valbellahorn 2	Wiesen	21.08.1989	Bürgin et al. (1991); herein
A/I 1924	Ducantal-Mannli-Schutthalde	Davos Sertig	1990	Bürgin et al. (1991); herein
A/I 1958	Gletscher Ducan 3	Stugl-Bergün	21.08.1991	Bürgin (1999); herein
A/I 2841	Gletscher Ducan 3	Stugl-Bergün	21.08.1991	Herein
A/I 2886	Gletscher Ducan	Davos Sertig	30.07.2003	Herein
A/I 2888	Ducanfurgga 4	Davos Sertig	1999	Herein
A/I 2889	Ducanfurgga 4	Davos Sertig	2000	Herein
A/I 2890	Gletscher Ducan	Davos Sertig	2000	Herein
A/I 3209	Ducanfurgga 3	Davos Sertig	17.07.1998	Herzog (2003); herein
BNM 201166	Val da Stugl-NE P. 2523	Stugl-Bergün	2021	Herein

terms fin rays, scutes, fulcra and its different types, procurrent rays, epaxial rudimentary rays, and principal rays follow definitions provided by Arratia (2008, 2009).

Phylogenetic analysis

A phylogenetic analysis was conducted to test the position of *Marcopoloichthys* among neopterygians. This analysis used the list of characters and matrix of Chen and Arratia (2022; Suppl. materials 1, 2), which is an expanded matrix of Xu (2020a) and has a large representation of neopterygian clades. *Boreosomus*, *Moythomasia*, and *Pteronisculus* were included in the outgroup. A second phylogenetic analysis was performed to test the position of *Marcopoloichthys* among teleosteomorphs. This analysis used the list of characters and matrix of Arratia et al. (2021; Suppl. materials 3, 4). *Australosomus*, *Bergeria* and *Polypterus* were used as outgroups. The phylogenetic analyses were conducted using PAUP* 4 (PAUP 4.0a169). All characters are unordered and unweighted.

Systematic paleontology

Superclass Actinopterygii Cope, 1887
Neopterygii Regan, 1923 sensu Xu (2020b)
Infraclass Teleosteomorpha Arratia, 2001

Family Marcopoloichthyidae Tintori et al., 2007

Emended diagnosis. The family diagnosis is based on a unique combination of characters (uniquely derived features among teleosteomorphs are identified with an asterisk [*]): Small fishes about 55 mm maximum length, with naked body, and highly modified protractile upper and lower jaws giving the anterior part of the head a characteristic profile [*]. The body shape is torpedo-like, with a head about 50% deeper than the caudal peduncle [*]. T-shaped mesethmoid with strong lateral processes. Two pairs of nasal bones [*]. Absence of supramaxillae [*]. Absence of dentition [*]. Preopercle L-shaped. Interopercle small triangle-like. Vertebral column with persistent notochord in older forms; chordacentral vertebral column in younger. Vertebral caudal region diplospondylous, with small interdorsal and interventral elements. Ossified ribs absent. Short, stout epineural processes associated to the abdominal neural arches. Large and curved pelvic plates. First dorsal fin proximal radial enlarged and plate-like, resulting from fusion of three or more radials and supporting four or more dorsal rays [*]. Enlarged last dorsal proximal radial supporting several dorsal rays [*]. First anal fin proximal radial basally expanded and very elongate and dorso-anteriorly bent, acting as post-coelomic bone [*]. Last anal fin proximal radial highly modified, expanded, and plate-like, supporting three or more lepidothrichia [*]. No fringing fulcra associated with paired, dorsal, or anal fins. Homocercal caudal fin with both lobes deeply forked. Body lobe of the caudal fin completely reduced. Ural region with five or six broad and short hypurals. Diastema hypural absent or very narrow. Caudal fin with dorsal and ventral scutes; well-developed epaxial and hypaxial basal fulcra; short series of epaxial and hypaxial fringing fulcra reaching about half length of first and last principal rays. Accessory fulcra present in hypaxial caudal lobe. Procurrent rays only present in the hypaxial lobe of caudal fin. Eighteen to 21 principal caudal rays. A few large scales around urogenital opening [*].

Content. One genus and four species known, *Marcopoloichthys ani*, *M. andreetti*, *M. faccii*, and *M. furreri* sp. nov.

Geographic distribution. Eurasian distribution, including Southern China (Yunnan and Guizhou Provinces), Northern Italy (Lombardy and Friuli), and eastern Switzerland (Canton Graubünden). Another undescribed species is present in the Middle Triassic of southern Switzerland, in Monte San Giorgio, Canton Ticino; T. Bürgin, pers. comm., 2022.

Age. From Anisian (Middle Triassic) to Norian (Late Triassic).

Genus *Marcopoloichthys* Tintori et al., 2007

Diagnosis. Same as family diagnosis.

***Marcopoloichthys furreri* sp. nov.**

https://zoobank.org/501280EA-CD8A-4464-96DE-C130D417D05C

Figs 2–14

1991 *Prohalecites* sp. Bürgin et al., p. 964, mention (for specimens PIMUZ A/I 1194 and 1924).

1999 Gen. et sp. indet. Bürgin, p. 487, fig. 8, mention (for specimen PIMUZ A/1 1958).

1999 Neopterygii *incertae sedis*. Bürgin, p. 494, app. 2, mention (for specimen PIMUZ A/1 1958).

2003 Halecostomi gen. et sp. indet. Herzog, p. 93, mention, text-fig. 29 and pl. 18/2 (for specimen PIMUZ A/1 3209).

Diagnosis. The species diagnosis is based on a unique combination of characters: The largest marcopoloichthyid reaching ca 55 mm maximum length. Skull roof covered with small and rounded oval tubercles and a few ridges of ganoine. Premaxilla and maxilla with slightly expanded articular region, spatulate-like and with crenulated anterior margin. Dentary ornamented with strong ridges and deep grooves; anterior margin covered with well-developed tubercles of different shapes. Short vertebral column with 33 to 35 vertebral segments, the first five fused into one element, the supradorsal carrier. With about nine supradorsal bones; the first five expanded distally, followed by sigmoid-shaped supradorsals; last supradorsal bones placed in front of the plate-like first compound dorsal proximal radial. Abdominal and first caudal neural arches with stout epineural processes reaching the next posterior neural arch. Dorsal fin support with first expanded proximal radial a massive squarish plate formed by fusion of four proximal radials. Last anal proximal radial with

long and distally expanded region supporting several lepidotrichia. Five hypurals; no hypural diastema present. Ten or 11 epaxial basal fulcra. Short series of epaxial fringing fulcra. Twenty or 21 principal caudal rays with straight segmentation. One to three short hypaxial procurrent rays; accessory hypaxial fulcra present. About 12 hypaxial basal fulcra. No urodermals present. With three or four large, ovoid scales associated with the urogenital region.

Derivation of name. The species name, *furreri*, honors Dr. Heinz Furrer who has dedicated most of his distinguished professional career to Triassic fossils of Switzerland, especially those of the Prosanto Formation.

Holotype. PIMUZ A/I 2886, an almost complete specimen, very well preserved (Fig. 2A) with a bent abdominal vertebral region; it was collected in Gletscher Ducan, Davos, in the Canton of Graubünden, Switzerland on July 30, 2003. Upper Prosanto Fm., Early Ladinian, Middle Triassic.

Paratypes. PIMUZ A/I 1194, TL about 23 mm; poorly preserved. PIMUZ A/I 1924, almost complete specimen, but it appears longitudinally compressed; poorly preserved. PIMUZ A/I 1958 almost complete, very well-preserved specimen from the same locality as holotype. PIMUZ A/1 2886, complete specimen: TL ca 50 mm. PIMUZ A/I 2888, incomplete, disarticulated specimen with well-preserved disarticulated pectoral girdle and fin. PIMUZ A/I 2889, incomplete specimen; anterior part of body, some abdominal vertebrae, pectoral and pelvic fins poorly preserved. PIMUZ a/1 2890, incomplete specimen missing part of head, paired fins, anal fin and posterior part of caudal fin. PIMUZ A/I 3209, an almost complete specimen of about 54.5 mm maximum length, with nicely preserved head and caudal fin. BNM 201166, almost complete specimen of ca 45 mm total length. See Table 1 for more information concerning specific specimens.

Type locality and age. Gletscher Ducan, Davos, in the Canton Graubünden, Switzerland. Upper Prosanto Fm., Early Ladinian, Middle Triassic. See Table 1 for information on localities and ages of specimens studied.

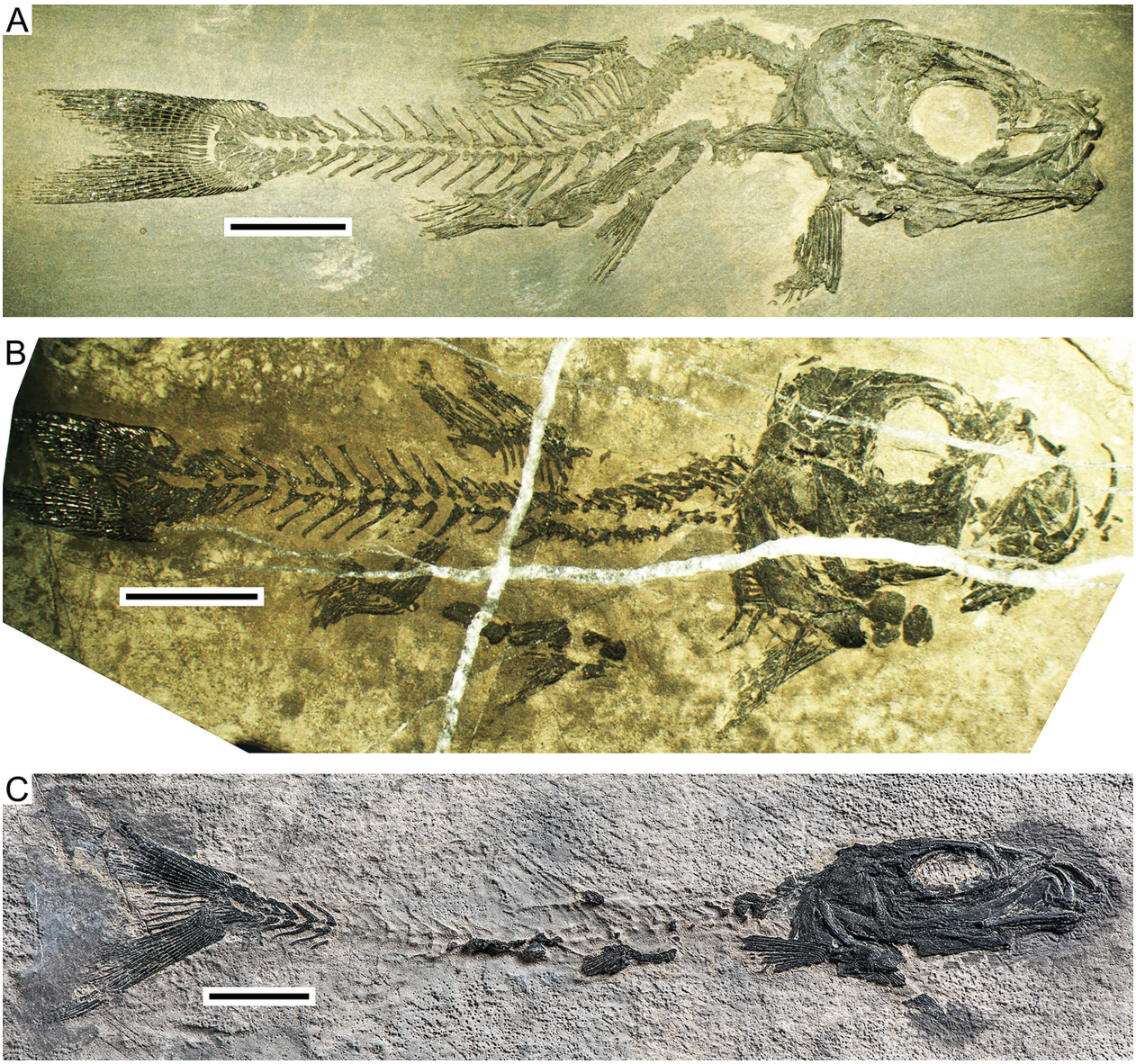

Figure 2. *Marcopoloichthys furreri* sp. nov. in lateral view. **A.** Holotype, PIMUZ A/I 2886; **B.** Paratype BNM 201166; **C.** Paratype PIMUZ A/I 3209. Scale bars: 5 mm. Photographs in **A** and **B** were taken by T. Scheyer and in **C** by C. Radke.

Figure 3. *Marcopoloichthys furreri* sp. nov. in lateral view. **A.** Paratype PIMUZ A/I 1958; **B.** Paratype PIMUZ A/I 2841. Scale bars: 5 mm. Photographs were taken by C. Radke.

Description. ***General description*.** The fish is ca 55 mm total length, slightly torpedo-like form (Fig. 2), with the head about three times deeper than the caudal peduncle. The dorsal fin insertion placed near to or at the midpoint of standard length (51–53% of SL). The pelvic fin insertion is placed at the same level of the dorsal fin insertion, but in one specimen is placed anteriorly (48–54%). The anal fin insertion is closer to the insertion of the pelvic fins than to the caudal fin (60–68% of SL); consequently, the fish has a long peduncle. The head is proportionally large, about 33 to 38% of standard length, and its aspect is very different when the mouth is closed compared to open. When the mouth is closed, most of the dorsal profile of the head looks gently rounded, decreasing in depth anteriorly (Fig. 3A; PIMUZ A/I 1958). When the fish is preserved in "feeding mode", the mouth is extended anteriorly, as well as the bones supporting the lower jaw, giving the head a characteristic profile (Figs 2C, 4; PIMUZ A/I 3209). The orbit is moderately large, about 28 to 39% of head length, and the preorbital region is moderately short, ca 25% of head length (specimens with closed mouth). The pectoral fins have a low position, closer to the ventral margin of the body than to the middle region of the flank (Figs 2, 3). The caudal fin is homocercal with both lobes almost the same size and with its posterior margin deeply forked. All exposed surfaces of cranial bones are ornamented with tubercles and longitudinal ridges covered with a thin layer of ganoine. The lateral surface of fin rays and fulcra is covered with a thin layer of ganoine. The body is naked, except for a few large scales (or scutes?) around the urogenital region, probably one in front of the dorsal fin, and dorsal and ventral scutes in the caudal fin.

***Skull roof and braincase*.** Although the skull roof is preserved in several specimens, it is almost impossible to trace each bone, because sutures are not visible due to fusion (Figs 4, 5). As the preservation permits, the bones of the skull roof apparently have smooth surfaces; however, under magnification, the bony surfaces may be densely ornamented with small, round or oval tubercles and short, longitudinal ridges (Fig. 5B). The ornamentation is covered by a thin layer of ganoine.

The parietal [= frontal] region is about 2.5–3 times longer than the postparietal [= parietal] region, and the limit between dermopterotic and postparietal cannot be traced (Figs 4, 5A, B). Consequently, it is assumed here that the postparietal and dermopterotic are fused to each other. This possibility is supported by the skull roof of the paratypes PIMUZ A/I 2887 and PIMUZ A/I 3209 (Figs 4, 5). According to available information, no specimen illustrates a complete fusion involving left and right sides of the skull roof, but each side is independent from its antimere.

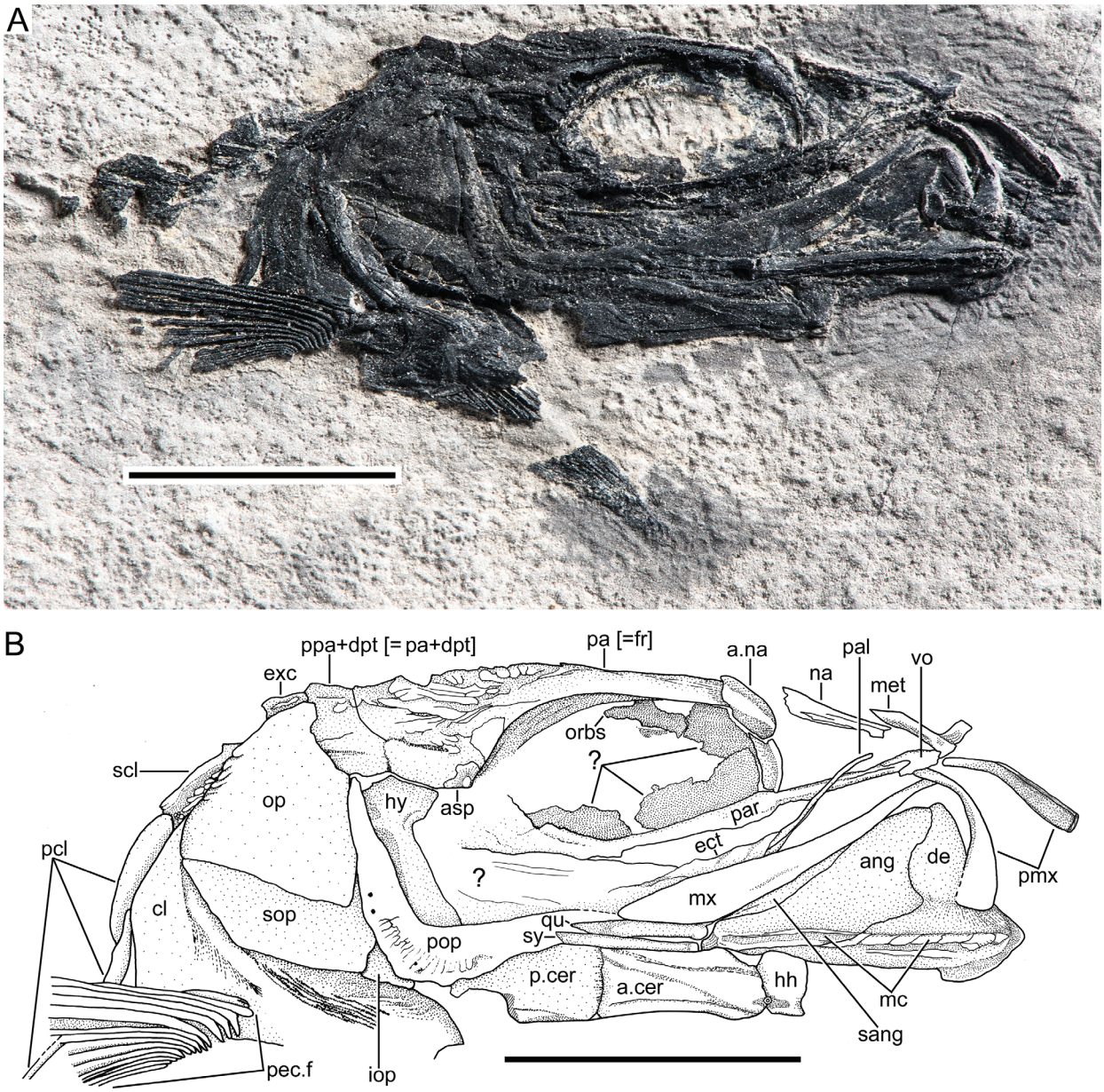

Figure 4. *Marcopoloichthys furreri* sp. nov. **A.** Photograph of right side of the skull roof of paratype PIMUZ A/I 2887 (photograph was taken by C. Radke); **B.** Interpretative drawing. Abbreviations: a.cer, anterior ceratohyal; a.na, accessory nasal bone; ang, angular; asp, autosphenotic; cl, cleitrum; de, dentary; ect, ectopterygoid; exc, extrascapular; hh, hypohyal; iop, interopercle; mx, maxilla; na, nasal bone; mc, mandibular canal; met, mesethmoid; mx, maxilla; pa[=fr], parietal [= frontal] bone; op, opercle; orbs, orbitosphenoid; pal, palatine; p.cer, posterior ceratohyal; par, parasphenoid; pcl, postcleitra 1–3; pec.f, pectoral fin; pmx, premaxilla; pop, preopercle; ppa+dpt [= pa + dpt], postparietal + dermopterotic bone; qu, quadrate; sang, surangular; scl, supracleithrum; sop, subopercle; sy, symplectic; vo, vomer; ?, uncertain or unknown. Scale bars: 5 mm.

From posteriad to rostrad, the skull roof is formed by the broadly and latero-ventrally expanded dermopterotic fused with the postparietal (postparietal + dermopterotic), which are densely covered with small tubercles (Fig. 5A, B). Apparently left and right bones are contacting each other through a straight suture (= *sutura harmonica*). It is unclear whether the parietal branch of the supraorbital canal extends into the compound bone, or the anterior middle pit-line is the one placed from the anterior margin to almost the half of the bone almost reaching the middle pit-line (Fig. 5B). The middle pit-line, as well as the anterior pit-line, are placed in conspicuous grooves. A posterior pit-line has not been observed. It is unclear if the supraorbital canal was covered by thin bone that collapsed after death and burial. The trajectory of the otic canal is not evident in the available specimens. The latero-ventral region of the postparietal + dermopterotic together with the autosphenotic are the main elements that articulate with the hyomandibula. Posterior to the postparietal + dermopterotic is a narrow, triangular bone that it is interpreted as an extrascapular (Fig. 5B). Although the extrascapular is incomplete in the available material,

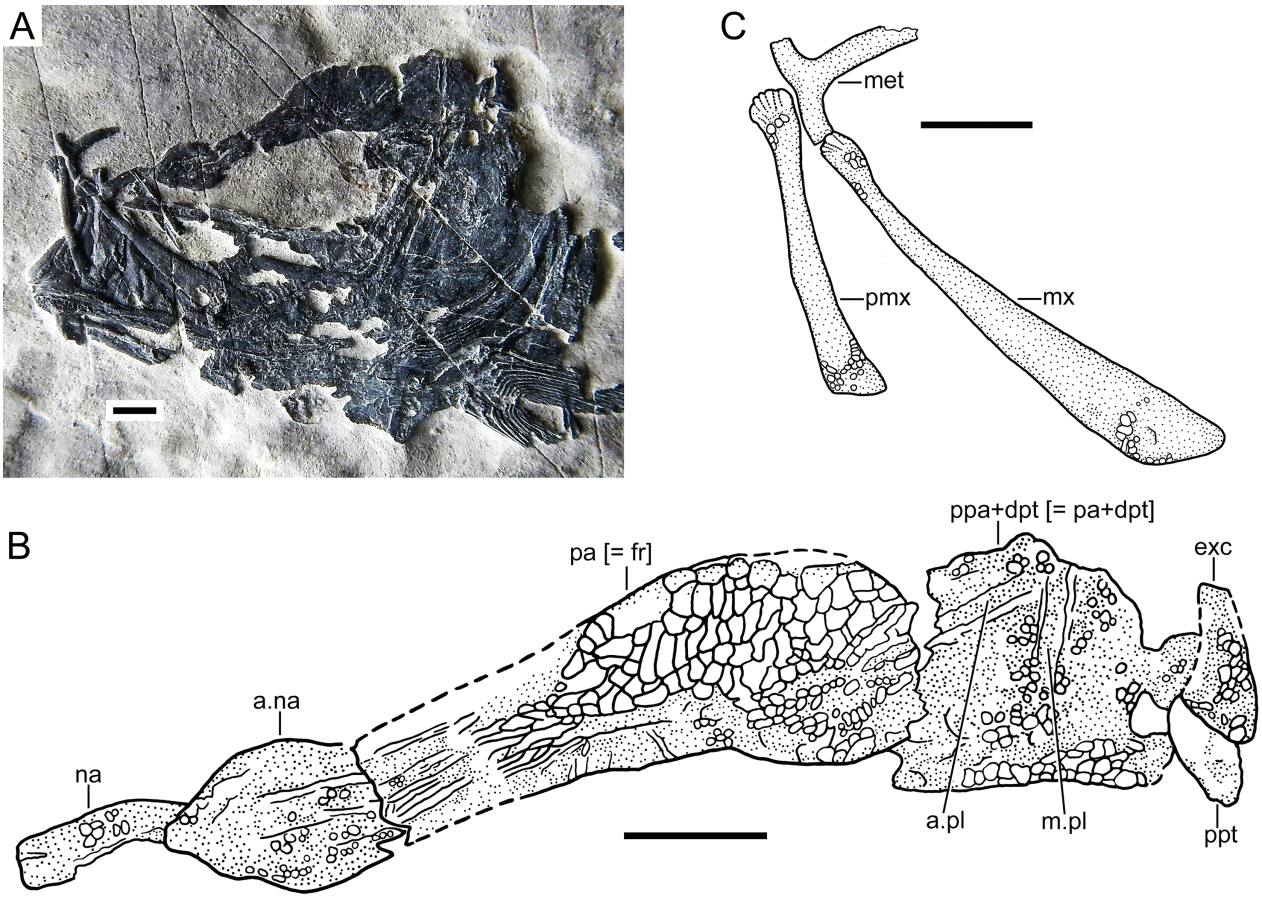

Figure 5. *Marcopoloichthys furreri* sp. nov. in lateral view illustrating some cranial bones in paratype PIMIZ A/I 2887. **A.** Cranium and pectoral girdle and fin in lateral view; photograph was taken by T. Scheyer; **B.** Skull roof bones illustrating ornamentation; **C.** Upper jaw bones; ornamentation on bones is damaged. Abbreviations: a.na, accessory or additional nasal bone; a.pl, anterior pit-line; exc, extrascapular; met, mesethmoid; m-pl, middle pit-line; mx, maxilla; na, nasal bone; pa[=fr], parietal [= frontal] bone; pmx, premaxilla; ppa+dpt [= pa + dpt], postparietal + dermopterotic bone; ptt, posttemporal. Scale bars: 1 mm.

it appears to be in contact, or at least becomes closer, to its antimere medially. The postero-median region of the skull roof is not preserved in any specimen, hence it is unknown whether a supraoccipital bone was present.

The short lateral process of the autosphenotic is well-ossified, but its dorso-lateral walls are not well preserved (Fig. 4). The autosphenotic seems to be fused with the postparietal + dermopterotic region posteriorly in the holotype (Fig. 2A), whereas it is not preserved in PIMUZ A/I 2887 (Fig. 5), which raises the possibility that the autosphenotic is not fused to any of its surrounding bones in this specimen.

The parietal [= frontal] is the longest bone of the skull roof, about twice the length of the postparietal + dermopterotic, and it ends just short of the postero-dorsal corner of the orbit; anteriorly it ends near the antero-dorsal corner of the orbit. Due to conditions of preservation, the interparietal [= frontal] and postparietal [= parietal] sutures are not discernable in most specimens, except for PIMUZ A/I 2887 that shows straight sutural borders (Fig. 5A, B). Because of the parietal preservation, it looks like a fontanelle was partially separating both left and right bones medially. The trajectory of the supraorbital canal is partially visible in PIMUZ A/I 2887 (Fig. 5), and no lateral sensory tubules or pores are observed. It is unclear whether the sensory canal was placed in a groove or whether the groove was covered by thin bone that has collapsed. The bones described above are part of the immovable region of the skull roof. In contrast, the so-called snout is formed by bones that are loosely articulated and changed position during the suction feeding process.

The anterior movable region of the skull roof includes, from posteriad to rostrad, an extra bone identified here as a posterior nasal or additional nasal, a nasal bone, and the mesethmoid (Figs 4A, A, 5A, B, 6, and 7). The first two are paired, whereas the latter is an unpaired bone. The additional nasal is a somewhat ovoid-shaped bone with slightly irregular anterior and posterior margins loosely articulated with the parietal posteriorly and the nasal bone anteriorly; when the fish is not feeding, this bone is placed downward, forming a kind of anterior margin to the parietal bone, and because of its position, it can be confused with the lateral ethmoid. This additional nasal is preceded by the nasal that is almost as long as the additional nasal in PIMUZ A/I 2887 (Figs 5, 6), but is about twice the length in the holotype (Fig. 6) and is almost rectangular-shaped. Unfortunately, its lateral margins are damaged in most specimens.

Both nasals seem to be loosely articulated medially. The supraorbital sensory canal is positioned almost in the mid-region of the additional nasal and nasal bones. Part of the surface of the nasal bone is covered by rounded tubercles in the holotype (Fig. 6). Forming the tip of the snout is a T-shaped median bone, the mesethmoid (Figs 4–7), with strongly ossified lateral processes, as well as a strongly ossified and elongate posteromedian process. There is no evidence of a rostral commissure. The holotype, PIMUZ A/I 2886, has an outstanding element preserved, which by comparison with some living atherinomorphs and cyprinodontiforms with suction feeding mechanisms, is interpreted as the rostral cartilage (Fig. 6). The rostral cartilage can be a continuous element extending in front of the parietal to the mesethmoid anteriorly. It can be perforated or not. In this case, only one ovoid foramen is observed, and because of this, I interpret that the rostral cartilage was broader, and its right side is incompletely preserved.

Morphologically, the anterior tip of the skull roof looks very different when the mouth is not open (e.g., Figs 5–7) compared to open (Figs 4, 7). When the mouth is closed, the anterior articular margin of the parietals together with the additional nasals produce a marked curved, downward region where the additional nasals lie. When the upper jaw is protracted, the profile of the anterior part of the head changes with the additional nasals, nasals, and mesethmoid placed almost in a straight line in front of the anterior margin of the parietal bones and the well-ossified lateral ethmoids. Since the mentioned bones are loosely connected, it is assumed here that the bones involved in the suction mechanism were kept in their position by the aid of ligaments and the rostral cartilage, but due to their soft structure, they were lost after death and burial.

The orbitosphenoid is not preserved in most specimens, but apparently both eyes are separated by an incomplete interorbital septum as shown by specimen PIMUZ A/I 3209 (Fig. 4). The lateral ethmoid is well-ossified and slightly bent, but its preservation does not allow a proper description.

The antero-middle region of the parasphenoid is visible in one of the fishes (Fig. 4), permitting its partial description. The parasphenoid is narrow anteriorly, it expands slightly posteriorly, and part of its ascendant process is poorly preserved just posterior to the orbital region. There are no teeth associated with the ventral surface of the bone or scattered below the parasphenoid. The parasphenoid joins anteriorly a small, narrow, triangular-shaped, and unpaired vomer (Fig. 4). No teeth are associated with the vomer either.

Orbit and circumorbital series. The fish has a moderately large orbit (Figs 2, 3A, 7), ranging from 28 to 39% of head length. When the fish was not feeding, the orbit was almost rounded, but when the fish was in feeding action, and the mouth protracted anteriorly, the orbit became oval-shaped.

The series of circumorbital bones is incomplete; supraorbital bones are absent dorsally, as well as an antorbital that seems to be missing at the antero-dorsal margin of the orbit in most specimens. Since I do not feel confident about the presence of an antorbital in this fish, I consider its presence uncertain. The infraorbital bones are thin and fragile and destroyed in most specimens. They are partially preserved in the paratype PIMUZ A/I 1958 (Fig. 2B); however, their delicate preservation makes their description difficult. Their total number is probably five plus a small dermosphenotic (Fig. 7). It is unclear whether the small flat bone placed between the dermosphenotic and

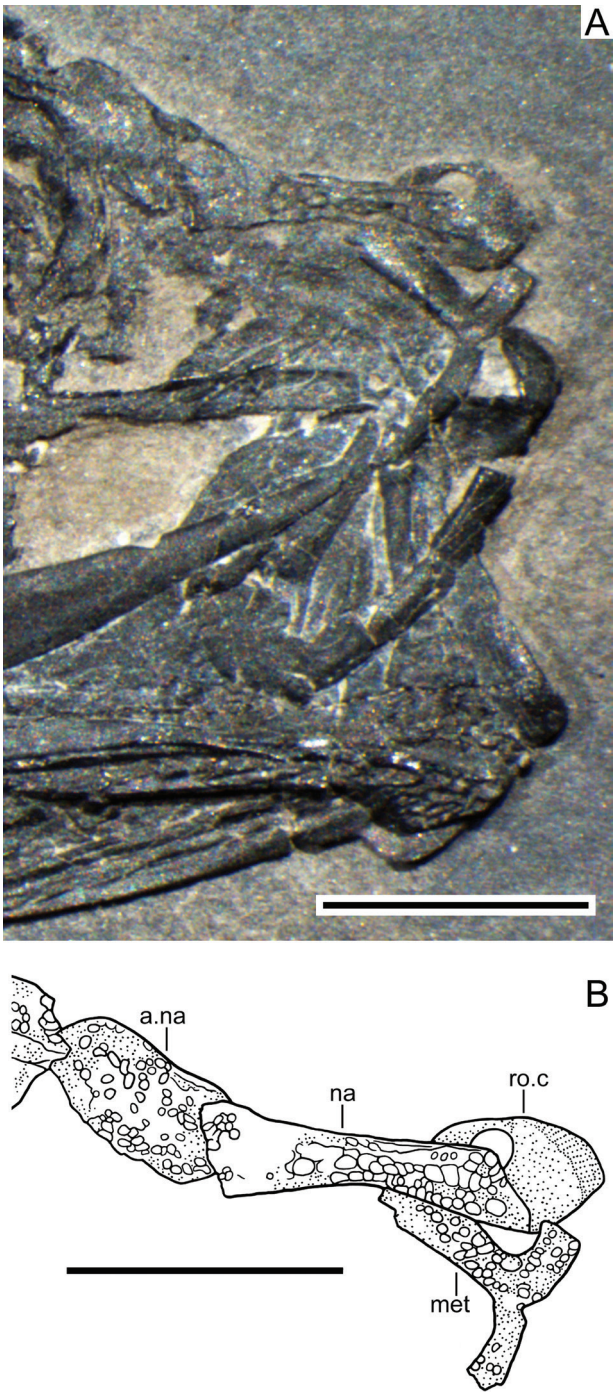

Figure 6. *Marcopoloichthys furreri* sp. nov. Anterior region of skull roof of holotype, PIMUZ A/I 2886. **A.** Photograph; it was taken by T. Scheyer; **B.** Interpretative drawing. Abbreviations: a.na, accessory or additional nasal; met, mesethmoid; na, nasal bone; ro.c, rostral cartilage. Scale bars: 2 mm.

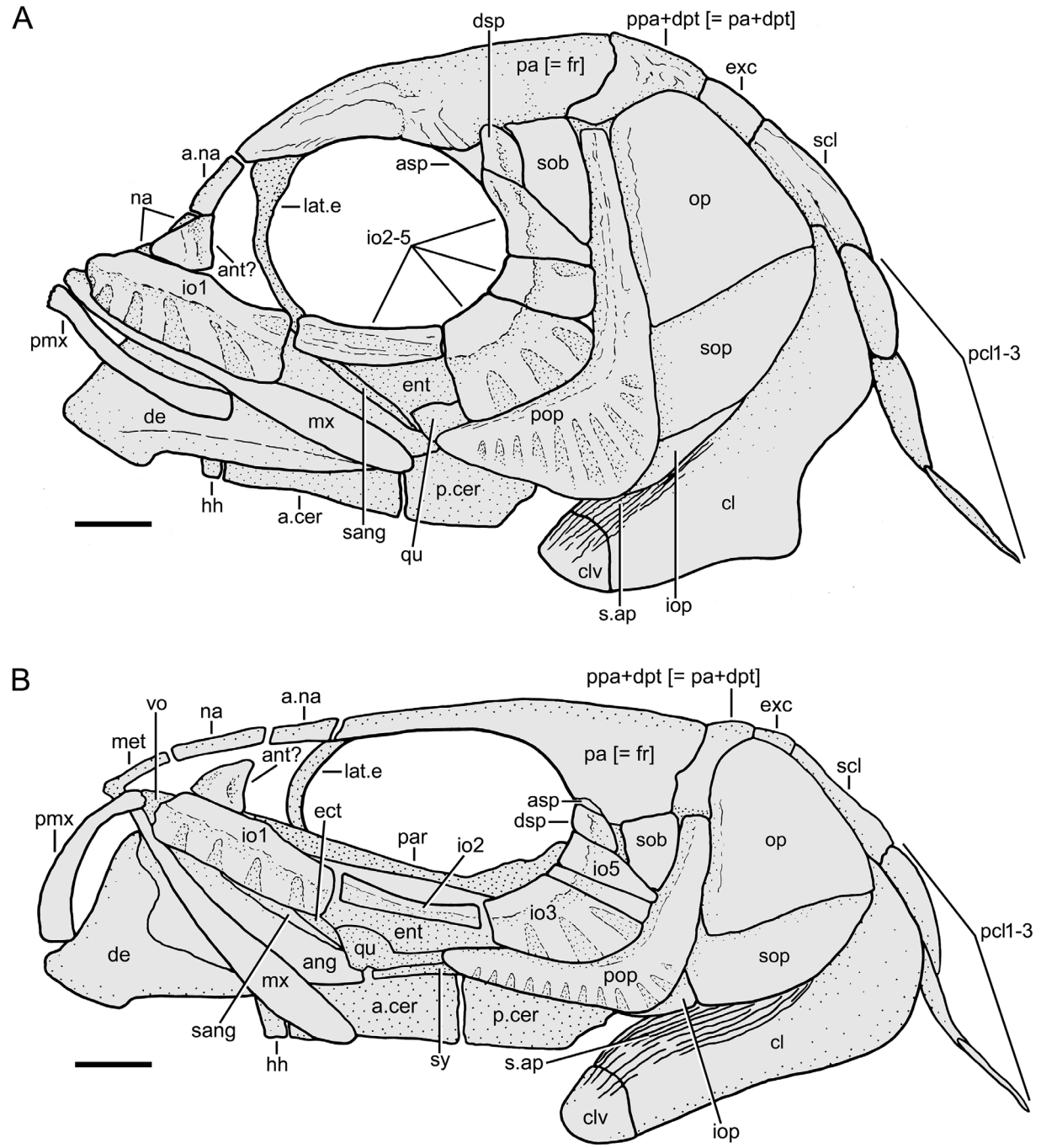

Figure 7. *Marcopoloichthys furreri* sp. nov. Restorations of head in lateral view. Heads reversed to the left. **A.** Fish during rest, based mainly on specimens PIMUZ A/I 1958, PIMUZ A/I 2841, PIMUZ A/I 2886; and BNM 201166; **B.** Fish during feeding, based mainly on specimen PIMUZ A/I 1958, PIMUZ A/I 2887; and BNH 201166. Abbreviations: a.cer, anterior ceratohyal; a.na, accessory or additional nasal bone; ant? antorbital?; asp, autosphenotic; cl, cleitrum; clv, clavicle; de, dentary or dentosplenial; dsp, dermosphenotic; ect, ectopterygoid; ent, entopterygoid; exc, extrascapular; hh, hypohyal; io1–5, infraorbitals 1–5; iop, interopercle; lat.e, lateral ethmoid; met, mesethmoid; mx, maxilla; na, nasal bone; op, opercle; pa [=fr], parietal bone [=frontal bone]; par, parasphenoid; ppa+dpt [= pa+dpt], postparietal bone + dermopterotic [= parietal bone + dermopterotic]; p.cer, posterior ceratohyal; pcl 1–3, postcleithrum 1–3; pmx, premaxilla; pop, preopercle; qu, quadrate; sang, surangular; s.ap, serrated appendage; scl, supracleithrum; sob, suborbital; sy, symplectic; vo, vomer. Scale bars: 1 mm.

anterior margin of the preopercle is a suborbital or part of the most dorsal infraorbital, but it is interpreted here as a suborbital.

Infraorbital 1 is the largest bone of the series, somewhat rectangular-shaped and with some broad sensory tubules that are difficult to count (Fig. 2B; PIMUZ A/I 1958); infraorbital 1 is incompletely preserved in PIMUZ A/I 2887, and the main infraorbital canal seems to be placed in a groove, but this could be misleading, since a groove is not observed in PIMUZ A/I 1958. Infraorbital

2 is an elongate, narrow bone, bearing a groove for the infraorbital canal (or the outer wall of the sensory tube is broken away). Infraorbital 3, at the posteroventral corner of the orbit, is slightly enlarged, reaching the anterior margin of the preopercle and its circumorbital margin, as well as that of the dorsal most infraorbital(s); it is well-ossified, and its few sensory tubules seem to be positioned in grooves. Infraorbital 4 is square-shaped, with its margin heavily ossified and with at least one sensory tubule. If a fifth infraorbital is present, it should be mainly represented by the thickened orbital margin. A description of the dermosphenotic is not possible because of poor preservation. The possible suborbital is a narrow, squarish bone dorsally and triangular-shaped ventrally, but this also could be the flat laminar surface of infraorbital 5. Unfortunately, there is not another specimen preserving the infraorbital series, so these uncertainties cannot be clarified with the available material.

In most specimens there are no orbitosphenoid or sclerotic bones preserved, and the orbital space looks "clean". It is uncertain whether this condition is the result of the preparation of this area, but one specimen (PIMUZ A/I 3209; Fig. 4) shows remnants of bones preserved. Due the flatness of the bones, it is unclear if these can be considered sclerotic bones or parts of a broken orbitosphenoid. In another specimen (Fig. 3A), there is one elongate bone at the anterior part of the orbit, giving the impression of the presence of an enlarged, slightly concave anterior sclerotic bone, but a possible posterior sclerotic is not preserved.

Upper jaw. Premaxilla and maxilla form the upper jaw. A supramaxilla has not been observed in any specimen, and it is assumed here to be absent. Both bones lack teeth, and their ventral margin is smooth. The premaxilla is about half of the length of the maxilla, and when the mouth is closed, the premaxilla is placed ventral to the ventral border of the maxilla, but when the mouth is open, both premaxillae project anteriorly in a very distinct position (compare Figs 2A and 3A with 2C and 4; and Fig. 7A with 7B).

The premaxilla (Figs 4, 5C) is a slightly bent bone, with its proximal end slimmer than the main section of the bone, which expands gently distally, ending in a straight margin. The slightly curved proximal region of the bone (Fig. 5C) lacks an ascendant process or any other process and is slightly spatulate, with a few short interdigitating ridges separated from each other by short grooves, giving this region a characteristic surface.

The maxilla (Figs 4, 5C) is an elongate bone, ending below the posterior half of the orbit and about the level of the articulation of the quadrate-lower jaw when the mouth is closed. It is narrower in its anterior half and slightly expanded at its anterior tip, with similar interdigitations as in the anterior tip of the premaxilla; in contrast, the maxilla expands gently posteriorly, keeping an elongate, straight aspect in its middle region, and then expands posteriorly, ending in a slightly triangular or rounded tip. A supramaxillary process is absent on the dorsal margin of the bone. The ventral margin is almost straight. The surface of the maxilla is covered with longitudinal bony ridges, which in some specimens retain remnants of ganoine. When the mouth is open, the maxilla is displaced anteriorly (compare Fig. 2A with Fig. 4 and Fig. 7A with 7B).

Lower jaw. The jaw (Figs 4, 8) is massive, relatively short, deep, and somehow triangular-shaped, with the quadrate-mandibular articulation placed below the posterior half of the orbit when the mouth is closed and displaced anteriorly, below the anterior half of the orbit, when the mouth is open (compare Figs 2A, 7A, 8 and 4, 7B). The jaw is formed laterally by three bones: dentary (= dentalosplenial or dentosplenial), angular, and surangular. Medially, an ossification interpreted here as a coronoid bone is present (Fig. 8). Since the medial view reveals only one bone posteriorly, it is assumed here that the angular, articular and retroarticular are fused into an angulo+articulo+retroarticular (Fig. 8). The lower jaw is toothless, and no evidence of sockets for teeth has been observed in any specimen.

The sutures between angular, surangular and dentary reveal that the dentary forms most of the jaw (Figs 7, 8). From a narrow but thick mandibular symphysis, the dentary expands abruptly dorso-posteriad, producing a massive and high coronoid process that is thicker and strongly ossified at its antero-dorsal region. The latter has a large contribution of the surangular. The antero-ventral portion of the dentary projects anteriorly and ventrally in a kind of flap or broad process (Figs 6A, 8) that commonly is broken, but it is well-preserved in A/I 3209 (Fig. 4). The postero-ventral process of the dentary narrows posteriorly and extends ventrally, almost reaching the posterior corner of the angular. A notch is absent in the ascending margin of the dentary. The surangular is an elongate bone, suturing ventrally with the dorsal region of the angular portion of the angulo + articulo + retroarticular and the postero-dorsal region of the dentary. The postarticular process is short.

The mandibular sensory canal is placed near the ventral margin of the jaw, and its trajectory is marked by a conspicuous ornamentation that has preserved remnants of ganoine. Sensory pores have not been observed in the postero-ventral region of the angulo + articulo + retroarticular, so it is assumed that the mandibular canal exits medially.

The lateral surface of the lower jaw of certain specimens presents a curious ornamentation at its antero-dorsal region of the dentary along the oral margin (Fig. 8). The ornamentation consists of well-developed, massive protuberances of various sizes and shapes that make the oral margin uneven. In other specimens such ornaments are missing (Figs 3A, 4, 6). It is unclear if these differences in ornamentation are sexual dimorphism, a hypothesis that should be tested when more specimens become available. The surface of the postero-ventral process of the dentary presents marked longitudinal ridges in most specimens; the deep ridges are also observed in the medial view of the jaw. Both the external protuberances and ridges are partially covered with a thin layer of ganoine.

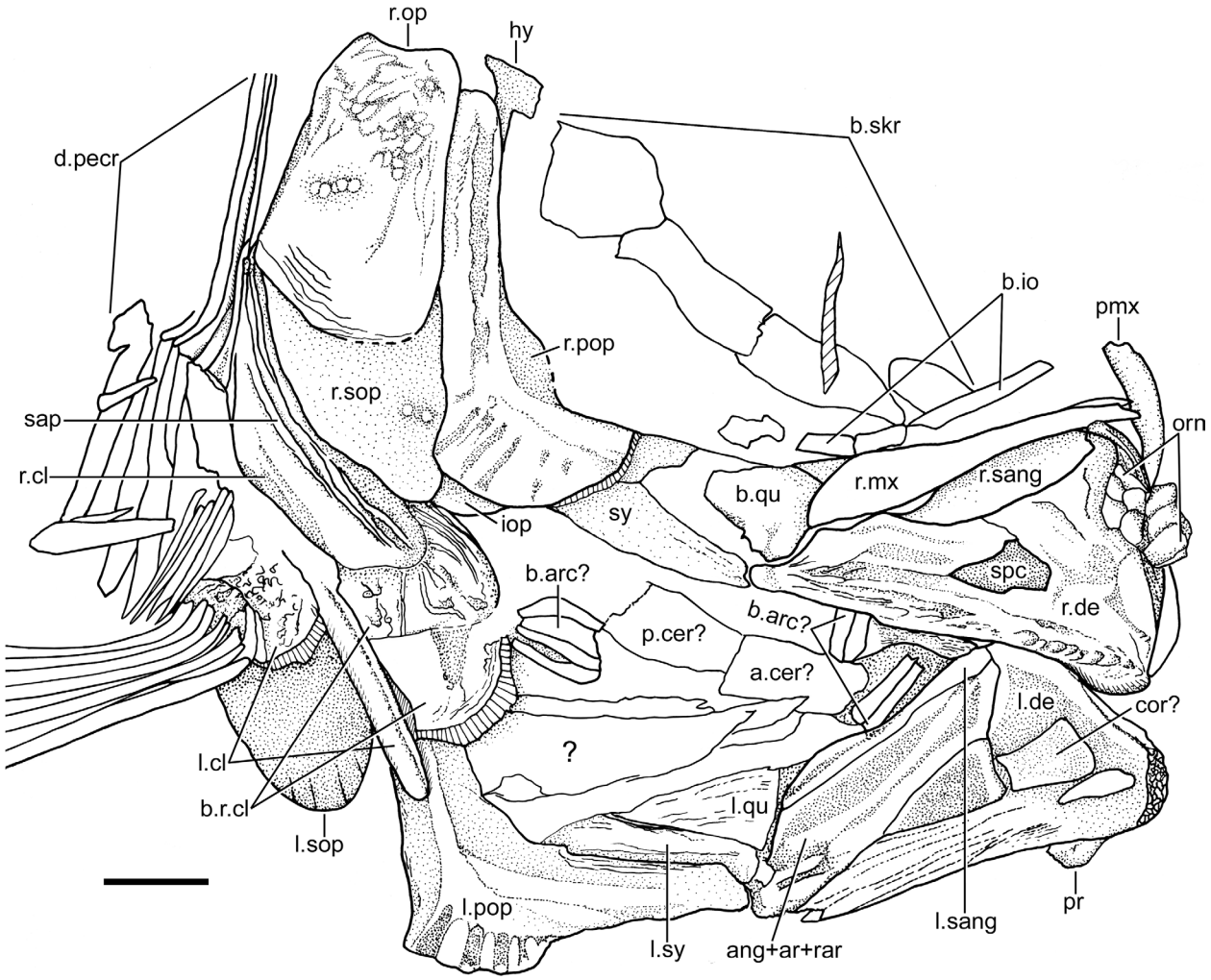

Figure 8. *Marcopoloichthys furreri* sp. nov., partially preserved cranium and pectoral girdle and fins in latero-ventral view of paratype, PIMUZ A/I 2841. Abbreviations: ang+ar+rar, angular+articular+retroarticular; b.io, broken infraorbital bones; b.arc?, broken branchial arches?; b.r.cl, broken anterior part of right cleithrum; b.qu, broken quadrate; b.skr, broken skull roof bones; cor?, coronoid?; d.pecr, displaced pectoral rays of left fin; hy, hyomandibula; iop, interopercle; l.cl, left cleithrum; l.de, left dentary; l.pop, left preopercle; l.qu, left quadrate; l.sang, left surangular; l.sop, left subopercle; l.sy, left symplectic; orn, ornaments; pmx, premaxilla; pr, ventral process of lower jaw; r. cl, right cleitrum; r.de, right dentary; r.mx, right maxilla; r.op, right opercle; r.pop, right preopercle; r.sang, right surangular; sap, serrated appendage; spc, space; sy, symplectic; ?, unidentified element. Scale bar: 1 mm.

The medial view of the lower jaw (Fig. 8) is somehow concave, with a deep triangular depression at the anterior confluence of the dentary and the angular portions. In some jaws, this region gives the impression of the presence of a space between bones. In front of the depression/space, a rectangular, well-ossified bone is positioned. Because of its position, I interpret this bone as a coronoid devoid of teeth.

Palatoquadrate, suspensorium, hyoid arch, and urohyal. Most of these elements are partially hidden by other bones or are destroyed so that the description is restricted to a few of them.

The regions where the metapterygoid, entopterygoid and ectopterygoid would be placed are damaged in most specimens, but a section of a bone that is interpreted here as the ectopterygoid is preserved in PIMUZ A/I 3209, anterior to the anterior margin of the quadrate (Fig. 4). Because of the size of the preserved areas, it is assumed here that the metapterygoid, as well as the entopterygoid, was a narrow bone. Another long, thin, and narrow bone anteriorly placed to the ectopterygoid is interpreted here as a palatine. Under the present conditions of preservation, it is impossible to clarify whether this is a dermal (dermopalatine) or a chondral bone (= autopalatine).

The quadrate is hidden by the anterior arm or ramus of the preopercle and the posterior region of the maxilla when the mouth is closed (Fig. 3A) and is partially exposed when the mouth is open, because the lower jaw displaces anteriorly (Figs 4, 7). The main body of the quadrate (Fig. 8) is slightly triangular close to its articular condyle with the lower jaw. The articular condyle is strong and slightly laterally projected to articulate with the lower jaw. The posterior margin of the quadrate, which shifts to a horizontal position in continuation with the jaw, when the mouth is open, is massive, and together with the symplectic, which lies ventrally to the quadrate,

provide a strong support for the lower jaw. The quadrate seems to continue posteriorly in a flat, almost rectangular process in the holotype, whereas the process ends in a sharp tip in PIMUZ A/I 3209 (Fig. 4). The complete length of the symplectic is unknown, because the bone is covered by the anterior margin of the preopercle or is broken, but considering its position and that of the hyomandibula, it is assumed here that it was a long bone. A quadratojugal has not been observed, and it is interpreted as absent.

The hyomandibula is incompletely preserved in all specimens, but in some its contour is visible throughout the preopercle. In specimen PIMUZ A/I 3209, it appears as a long, columnar bone that is inclined ventro-anteriorly when the mouth is open, and together with the long symplectic gives support to the jaw; the hyomandibula is placed in an almost straight line when the mouth is closed. Its dorsal region articulating with the cranium is broader and well-ossified and continues ventrally as a well-ossified shaft; it is unclear whether an anterior membranous flange is present or not. The dorsal articular region of the hyomandibula (Fig. 4) apparently has only one elongate articular condyle with the latero-ventral articular facets of the dermopterotic and autosphenotic regions laterally. Nothing can be said about the opercular process. Considering the length of the jaw and the position of the quadrate-mandibular articulation, the symplectic is assumed to be a long and strong bone that is partially exposed in PIMUZ A/I 3209 and PIMUZ A/I 2841; an alternative possibility is the presence of an elongate cartilaginous articular region filling the space between the ventral margin of the hyomandibula and the dorso-posterior margin of the symplectic.

The lower part of the hyoid arch preserves a posterior ceratohyal (Fig. 4C, D) that is almost as long as the anterior ceratohyal, which is an almost rectangular bone, lacking a foramen or a notch close to its smooth, dorsal margin. Only one massive, squarish hypohyal articulating with the anterior margin of the anterior ceratohyal (Fig. 4C, D) is present. A urohyal has not been observed in any specimen, and it is assumed here to be absent.

Opercular and branchiostegal series, and gular plate. Although the preopercle is an element associated with the suspensorium, it is included here to describe the opercular series together. The preopercle (Figs 2C, 3A, 4, 8) is a large and L-shaped bone, which is slightly expanded postero-ventrad. The dorsal lobe is slightly longer than the ventral one when the mouth is closed (PIMUZ A/I 1958); however, when the mouth is open, the angle of the preopercle changes, and both arms are about the same length (Figs 4, 7B). Its dorsal arm is about 57% longer than the ventral one, almost reaching the ventro-lateral margin of the dermopterotic region. When the mouth is closed, both arms form an almost right angle, whereas the angle increases to over 100 degrees when the mouth is open, as a result of the anterior extension of the mouth and the action of assumed ligaments joining the posterior margin of the lower jaw and the anterior margin of the anterior arm of the preopercle and interopercle. The preopercle has a gentle flange just anterior to the confluence of both arms where a curvature of the preopercular canal is present. A notch at the posterior margin of the bone is absent. The preopercular canal (Fig. 8) apparently only bears the main preopercular canal, because no tubules are conspicuous at is dorsal arm. A few tubules (Figs 3A, 4, 7, 8) fill the preopercular ventral arm; more precise information is not available because of incomplete preservation of the available preopercles. The sensory tubules are delicate, simple and narrow, and open irregularly near to or at the ventral margin of the bone.

The opercle (Figs 3A, 4, 8) is not very well preserved in the available specimens, but still, it is possible to observe that is the largest element of the series, slightly deeper than broad, and slightly narrower at its dorsal margin, whereas the ventral margin is slightly broader. Dorsally, the opercle reaches the latero-ventral margin of the dermopterotic region, the extrascapular and the posttemporal, and posteriorly, the supracleithrum and cleithrum. Its dorsal and anterior margins are almost straight, whereas the posterior margin in gently curved, and the ventral margin is markedly oblique. Anteriorly, the margin of the opercle is thickened and joins the dorsal limb of the preopercle, whereas it joins the subopercle postero-ventrally and the interopercle antero-ventrally. The opercular surface is irregularly covered with short ridges and rounded and oval tubercles. The subopercle (Figs 3A, 4, 8) is large, as broad as the opercle, and slightly shorter. The general aspect of the bone is not easy to describe, because it is gently curved ventrally in some and markedly rounded in others. Information on the size of the antero-dorsal process is not possible based on the available specimens. A small interopercle (Figs 4, 8) is partially covered by the postero-ventral margin of the preopercle so that its complete shape and size remains unknown.

Branchiostegal rays are not preserved, except for one specimen (holotype PIMUZ A/I 2886) with two narrow and spine-like posterior branchiostegals associated with the posterior ceratohyal. The absence of branchiostegals or their low number in one specimen could simply indicate that the fish has very few that are usually not preserved. Only one short and rounded branchiostegal ray was mentioned and illustrated for *Marcopoloichthys ani* by Tintori et al. (2007: p. 16, fig. 3). A gular plate has not been observed, and it is assumed here that it is absent.

Vertebral column, intermuscular bones, and ribs. The information on the whole vertebral column is incomplete, because most specimens provide partial or no information. An almost complete vertebral column is preserved in several specimens, including the holotype (PIMUZ A/I 2886; Fig. 2A) and paratypes (BNM 201166 and PIMUZ A/I 19568; Figs 2B, 3A), while the caudal region is well-preserved in PIMUZ A/I 2890 and several other specimens.

The vertebral column is aspondylous (see Arratia et al. 2001 for different types of the vertebral column), with well-developed arcocentral elements forming the centra,

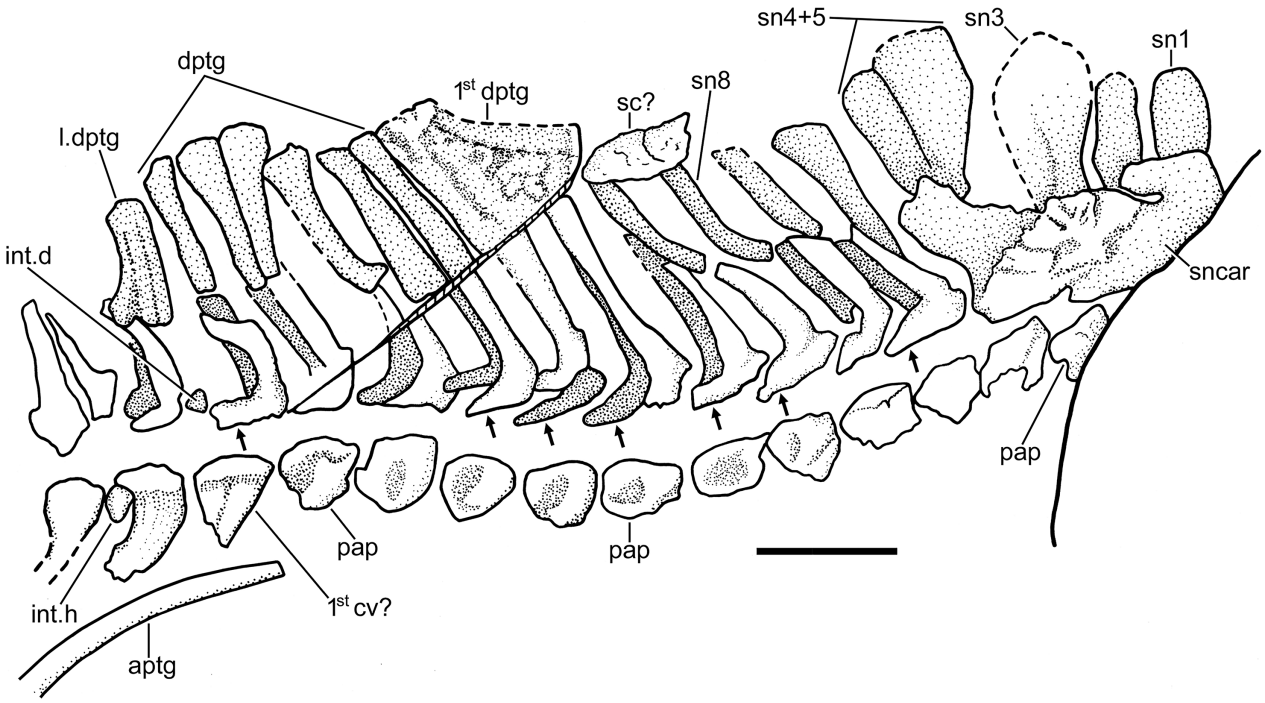

Figure 9. *Marcopoloichthys furreri* sp. nov., illustrating a lateral view of the abdominal or precaudal region of the vertebral column and associated elements and the dorsal fin and endoskeletal support (paratype PIMUZ A/I 1958). Small arrows point to the epineural processes. Abbreviations: aptg, 1st anal pterygiophore or proximal radial; dptg, dorsal pterygiophores or proximal radials; int.d, interdorsal arcocentrum; int.v, interventral arcocentrum; l.dptg, last dorsal pterygiophore; pap, parapophyses; sc?: scale or scute?; sncar, supraneural carrier; sn1–8, supraneurals 1–8; 1st cv?, first caudal vertebra?; 1stdptg, first dorsal pterygiophore or fused proximal radials. Scale bar: 1 mm.

but the notochord remains persistent and functional in adults. There are about 33 to 35 vertebral segments, including those of the hypurals. About 13 to 18 are abdominal, monospondylous vertebral segments, whereas the caudal region is diplospondylous, with very small interdorsal and interventral arcocentral elements alternating with the well-developed basidorsal and basiventral arcocentral elements. Because of their small sizes, many of the interdorsal and interventral elements have not been preserved. No remains of centra are present in the ural region.

The first five neural arches and spines are fused into one special, previously unreported element that is preserved in the holotype PIMUZ A/1 2886, as well as in PIMUZ A/1 1958 (Figs 2, 3, 9). This compound bone is named here "supradorsal carrier" and is formed by the lateral, fused expansions of the neural arches and hemispines of the first abdominal vertebrae, forming two lateral wings (Fig. 9). Five supraneurals are in a median position between the two lateral wings of the supradorsal carrier. I expect that this special structure is a synapomorphy of marcopoloichthyids, a character that should be checked in other species when better-preserved material becomes available.

There are about 13 or 14 parapophyses (Figs 3, 9), the first ones covered by the opercle and the dorsal bones of the pectoral girdle. The parapophyses are comparatively large for the size of the fish, and they are well-ossified; they are squarish in shape and each bear a small cavity close to its ventral margin. No ribs are preserved in the available material, and they were not reported or illustrated in *Marcopoloichthys ani* (Tintori et al. 2007: fig. 4) either; thus, it is accepted here that marcopoloichthyids do not have ossified ribs.

The neural arches of the abdominal vertebrae (Figs 3, 9) are slightly expanded, and the halves of each arch, plus their elongate neural spines, are unfused medially. The lateral wall of each neural arch projects in a stout and short epineural process (= epineural bone; see Arratia 1997 or 1999 on the terminology) emerging at the postero-lateral margin of the arch. They are easily broken because of their position and structure.

The neural arches of the first caudal vertebrae (Figs 2, 3A, 9) are slighter broader than those of the abdominal vertebrae, and each has an epineural process until the third or fourth vertebra posterior to the last anal pterygiophore. The neural and haemal spines of the caudal region are narrow, except for those of the preural centra (see below). The neural and haemal spines are moderately inclined toward the body axis in the precaudal region, increasing their inclination caudally (Figs 10, 11). The first haemal spines (Figs 10, 11) are short, not extending between the anal pterygiophores or just reaching them. The neural and haemal spines of the mid and caudal regions are ossified, showing an internal core of cartilage where the bones are broken.

The series of supraneural bones is commonly not preserved, distorted, or covered by other structures. The series is formed by nine bones in the paratype (PIMUZ A/I 1958), with the first five associated with the supradorsal carrier. These anterior supradorsals are slightly ovoidal and expanded, especially supraneural 3, whereas supraneural 4 and 5 are partially fused proximally. The

subsequent supradorsals are slightly sigmoid-shaped. The series extends up to the expanded, plate-like, compound first dorsal proximal radial, and it does not extend between the most anterior proximal radials as in *Marcopoloichthys ani* (Tintori et al. 2007: fig. 4).

The epineural processes of the neural arches (Figs 9, 11) extend along the abdominal region, ending posterior to the last dorsal pterygiophore. The broad and well-ossified epineural processes are short, extending laterally on the neural arch of the next vertebral segment. Epipleural bones are absent.

Pectoral girdle and fins. The pectoral girdle includes dermal and chondral bones. The dermal bones are the posttemporal (linking the girdle with the cranium), supracleithrum, cleithrum, and postcleithra. It is unclear whether a clavicle was present, but see below. The chondral bones are the scapula, coracoid, and proximal and distal radials. The posttemporal is incompletely preserved in the available material (Figs 4, 5B). Apparently, it is a relatively small and narrow bone, placed laterally to the extrascapular; it is unclear whether a dorsal process for articulating with the cranium is present. The main lateral line is not observed.

The supracleithrum (Figs 4, 7) is incompletely preserved or covered by the opercle, but it seems to be an elongate bone. The trajectory of the lateral line is not observed. The sigmoidal-shaped cleithrum (Figs 4, 5A, 7–9) is a heavily ossified bone, with a moderately long dorsal limb and markedly developed, expanded and curved ventral limb, which is partially broken in the available material, making identification of its complete area difficult. The cleithrum is slightly expanded at its postero-dorsal corner and becomes narrower at its dorsal region. The anterior surface of the cleithrum is covered by a long and broad serrated appendage that is almost completely preserved in the paratypes PIMUZ A/I 2841 and 2887 (Figs 5A, 8). The external surface of the cleithrum in PIMUZ A/I 2888 (Fig. 10) is abraded so that the serrated appendage is not preserved. A broad clavicle in front of the antero-ventral region of the cleithrum is observed in specimen BNM 201166.

Three postcleithra are present (Figs 4, 7). Postcleithrum 1, the uppermost element of the series, is elongated, with a slightly rounded posterior margin. Dorsally, it articulates with the supracleithrum and anteriorly with the upper part of the cleithrum and ventrally with postcleithrum 2. Postcleithrum 2 is slightly narrower than postcleithrum 1 and is curved postero-distally. Postcleithrum 3 is a splint-like bone. By comparison with other teleosteomorphs, it is assumed here that the three bones were not externally placed, but they were covered by the body hypaxial musculature.

The scapula and coracoid (Fig. 10) are incompletely preserved in the available material, and they are not informative. Four proximal radials are observed in the paratype PIMUZ A/I 2888 (Fig. 10), with the first two being larger than the third and fourth proximal radials, which are square-shaped. At least three small distal radials are preserved between the broken proximal region of some pectoral rays.

The pectoral fin (Figs 2, 3, 5A) is positioned near the ventral margin of the body. The total number of pectoral rays is unknown, because commonly the fins are incomplete, but 15 rays are preserved in the right fin in PIMUZ A/I 2841, and most fins in other specimens have ca 12 rays preserved. All rays have very long bases, are scarcely branched, and segmented distally; a few last rays, closer to the body, are smaller than the lateral ones. The first pectoral ray, which is exposed in PIMUZ A/I 2888 (with the pectoral girdle and fin displaced), merits a description. The first ray is a massive ray formed by the fusion of three rays at least (Fig. 10). These rays are fused at their

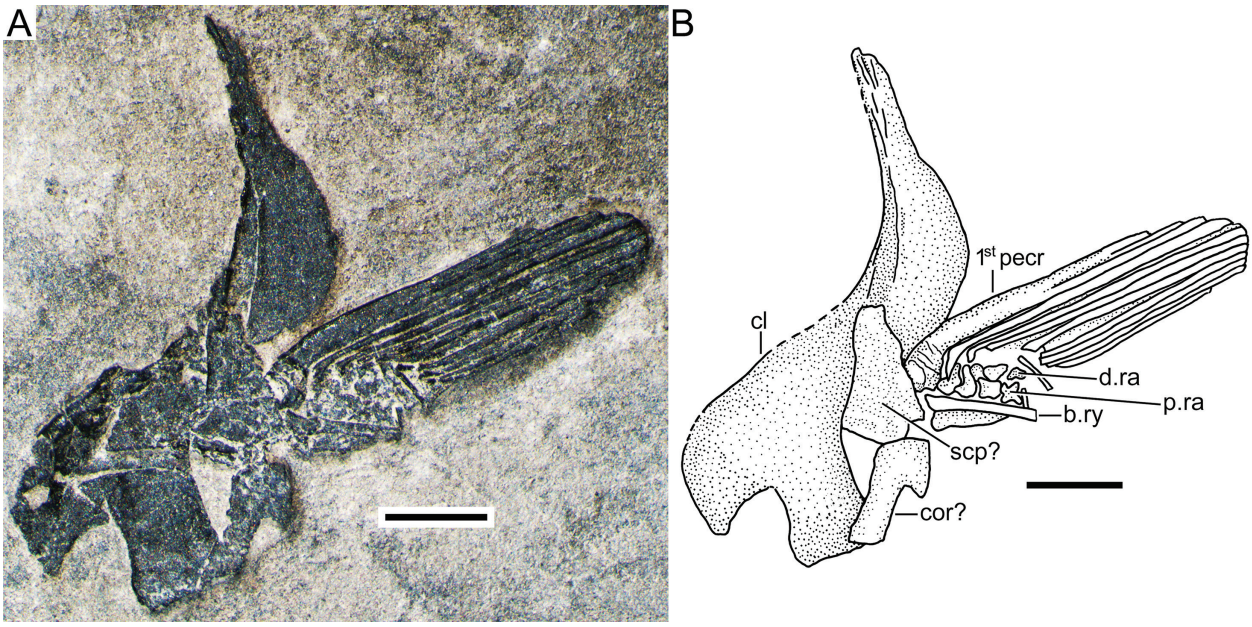

Figure 10. *Marcopoloichthys furreri* sp. nov., illustrating part of the pectoral girdle and fin (paratype PIMUZ A/I 2888). Abbreviations: b.ry, broken ray; cl, cleithrum with antero-ventral part broken; cor?, coracoid?; d.ra, distal radials; p.ra, proximal radials; scp?, scapula?; 1st pecr, first pectoral ray. Scale bars: 1 mm.

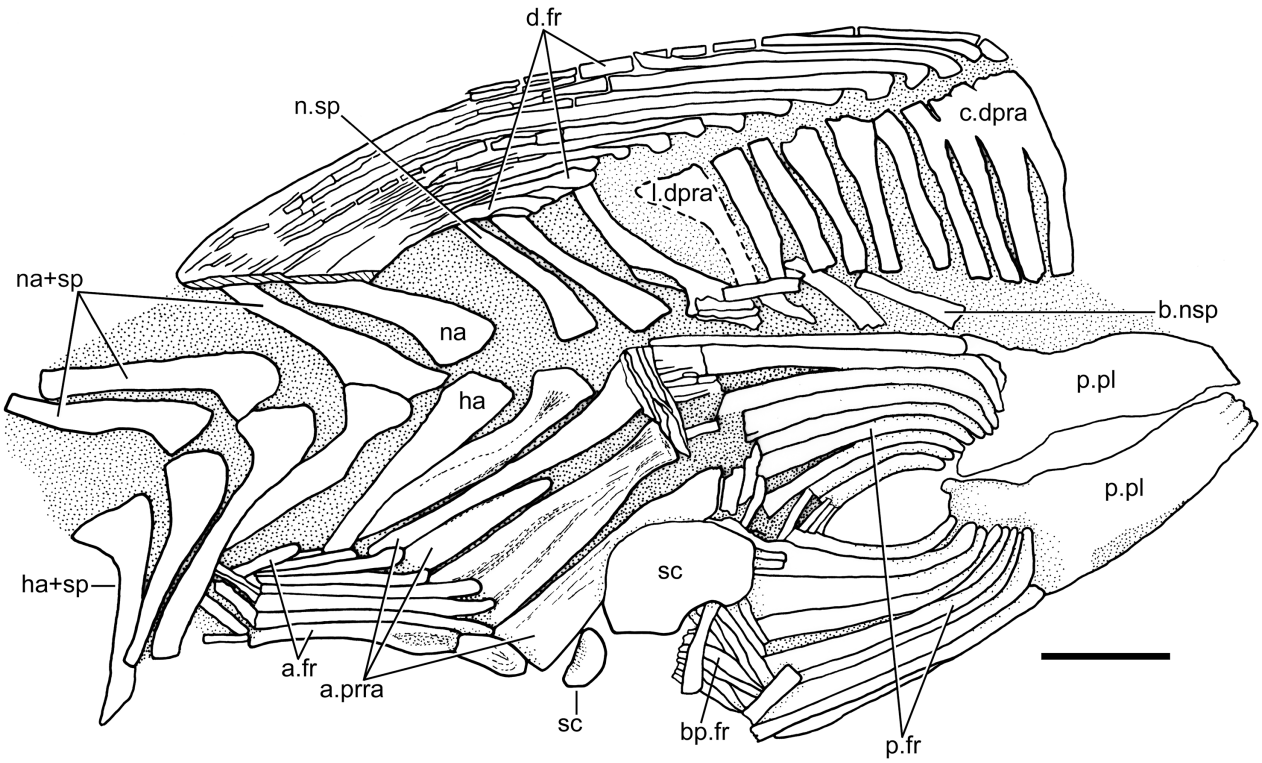

Figure 11. *Marcopoloichthys furreri* sp. nov., illustrating the dorsal, anal, and pelvic fins and associated structures (paratype PIMUZ A/I 2841). Abbreviations: a.fr, anal fin rays; a.prra, anal proximal radials; bp.fr, broken pelvic rays; b.nsp, broken neural spines; c.dpra, compound dorsal proximal radial element; d.fr, dorsal fin rays; ha, haemal arch; ha+sp, haemal arch plus spine; l.dpra, last dorsal proximal radial; na, neural arch; na+sp, neural arch plus spine; n.sp, neural spine; p.fr, pelvic rays; p.pl, pelvic plate or basipterygium; sc, scales. Scale bar: 1 mm.

bases, being separated distally. This first compound ray is slightly expanded and thicker at its proximal portion where the propterygium is fused with its base.

Pelvic girdles and fins. The pelvic girdles are partially exposed in several specimens (Figs 2A, B, 3A, B, 11). A large, elongate plate-like basipterygium (or pelvic plate) is slightly curved medially, with its lateral margin more strongly ossified than the rest of the plate. The posterior part of the basipterygium is slightly broader than the anterior margin and presents a short postero-medial process. The number of rays per fin are difficult to count, due to preservation. Ten or 11 rays are present in the holotype; eight of them are thicker and longer than the two or three medial rays. In contrast, nine long pelvic rays are preserved in each fin in specimen PIMUZ A/I 2888. Eleven rays were mentioned for *Marcopoloichthys ani*, but the number of rays remains unknown for *M. andreetti* and *M. faccii* (Tintori et al. 2007). The pelvic rays of *M. furreri* sp. nov. have long bases, are distally segmented, and apparently branched only once. This information is collected from the holotype, with one ray distally exposed (Fig. 2A). In other specimens, the distal parts of the fin rays are disarticulated or overlapping so that they are not informative (Fig. 11). Because of the position of the articular region of each ray, it is unknown whether proximal radials were present.

Dorsal fin and radials. The dorsal fin (Figs 2, 3, 11, 12) is commonly not well preserved with its rays partially displaced or damaged so that a precise total number of dorsal fin rays cannot be provided, but considering that the paratype PIMUZ A/I 2841 has 15 rays preserved, including a short, thin one segmented anteriorly, this could indicate that the fin has ca 15 rays.

Commonly, the dorsal pterygiophores preserved the proximal radials, however in the holotype, some of the anterior middle and distal radials are also preserved (Fig. 12). The series of proximal radials presents distinct features characterizing marcopoloichthyids, for instance, the modifications in the first and last proximal radials. In *M. furreri* sp. nov., the first proximal radial can be plate-like and square, but in others, the proximal radials are incompletely fused so that the elements forming this complex structure can be counted (Fig. 11). There are six intermediate proximal radials followed by one modified last radial bearing an undetermined number of rays in PIMUZ A/I 2841 and holotype (Figs 11, 12). This last proximal radial has an expanded distal articular region that projects ventrally in a narrow, markedly curved process. The complex plate-like first proximal radial in *Marcopoloichthys ani* is ax-shaped, whereas it is pear-shaped in *M. andreetti* (Tintori et al. 2007); in addition, *M. ani* has an ax-shaped proximal radial and nine to 10 proximal radials posterior to the first, which is a higher number than in *Marcopoloichthys furreri* sp. nov.

Anal fin and radials. The anal fin and its pterygiophores are not well preserved in the available material, and because of this, a description is difficult, and a total

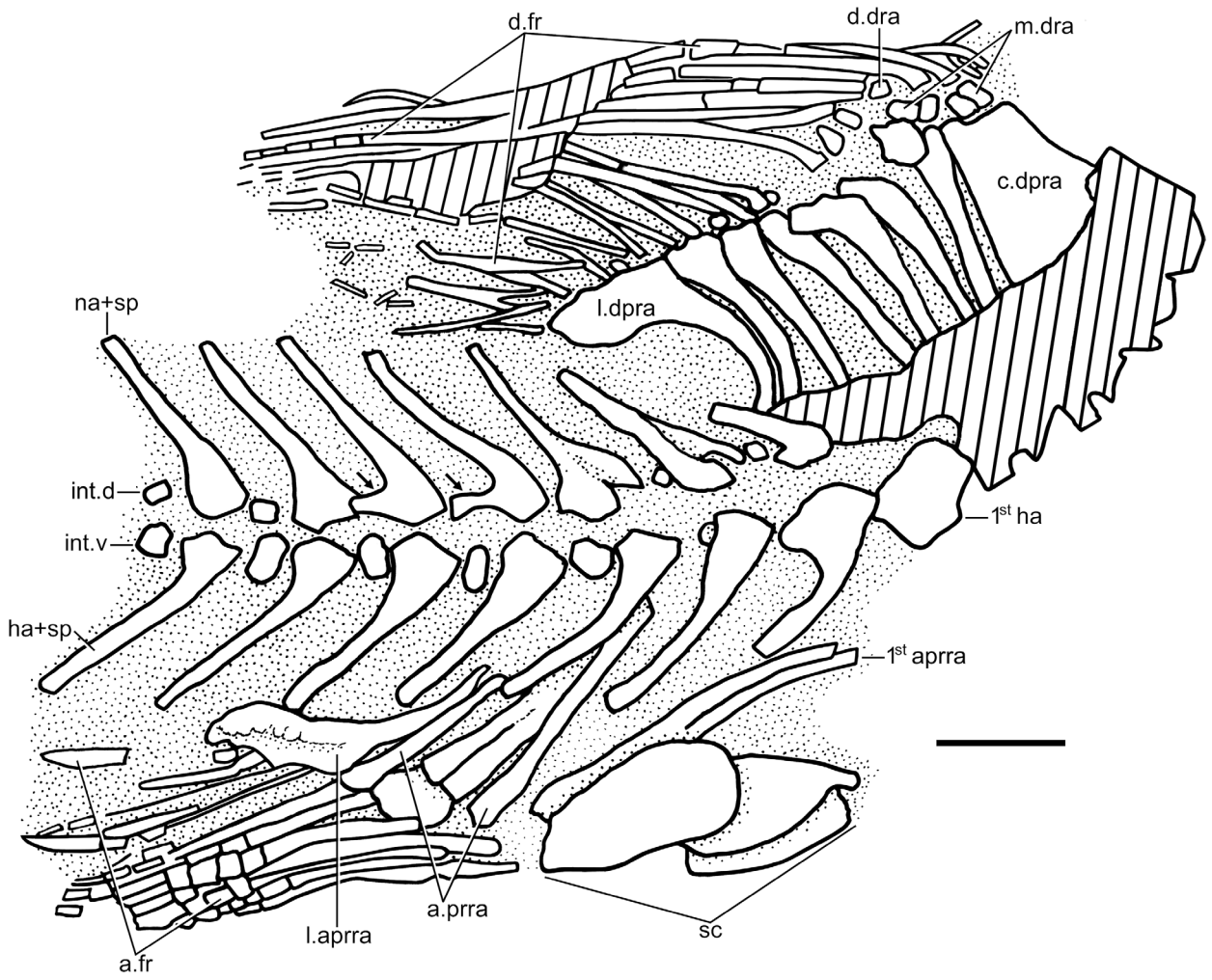

Figure 12. *Marcopoloichthys furreri* sp. nov., illustrating the dorsal, anal, and pelvic fins and associated structures (holotype PIMUZ A/I 2886). Oblique lines represent damaged areas. Abbreviations: a.fr, anal fin rays; a.prra, anal proximal radials; c.dpra, compound dorsal proximal radial element; d. dra, distal dorsal radial; d.fr, dorsal fin rays; ha+sp, haemal arch plus spine; int.d, interdorsal element; int.v, interventral element; l.aprra, last anal proximal radial; l.dpra, last dorsal proximal radial; m.dra?, middle dorsal radial; na+sp, neural arch plus spine; sc, scales; 1st aprra, first anal proximal radial; 1st ha, first haemal arch. Scale bar: 1 mm.

count of fin rays is not available. Additionally, there is variation in the number and amount of fusion of the proximal radials. The most complete series of proximal anal radials, or the most informative, is that present in the holotype (Fig. 12). In this specimen, the first anal proximal radial is a compound element resulting from the incomplete fusion of two proximal radials. This first element curves antero-dorsally giving the radial a characteristic shape, reminiscent of the postcoelomic bone of pycnodontiforms (Tintori et al. 2007). The first anal proximal radial is followed by a second, long, narrow radial, that is followed by a third element that results from the partial fusion of two proximal radials which are broken at their bases. Behind this element is one simple proximal radial that is followed by the last radial. The last radial is an elongate element bearing a narrow, thin anterior process that extends dorsally between the distal tips of the haemal spines and has a broad distal portion for articulation with several lepidotrichia (Fig. 12). In total, the anal series of proximal radials in the holotype included five separate elements. In the paratype PIMUZ A/I 2841, only three proximal radials are preserved, and the first and last are not preserved.

Caudal fin and endoskeleton. The caudal fin and endoskeleton are preserved in several specimens, but the dorsal elements of the ural region are poorly or not preserved at all. The homocercal caudal fin (Figs 2, 3) is deeply forked, with few short middle principal rays compared to the long first and last leading marginal ray that frame the segmented and branched principal rays. Many rays preserve a thin layer of ganoine.

One or two preural vertebrae support the most anterior basal fulcra. The preural vertebrae, as well as the ural ones, are supported by a functional notochord. Consequently, except by the arcocentra, no centra are formed, and the region is monospondylous, in contrast to diplospondylous vertebral segments in anterior and mid-caudal vertebrae (Figs 2, 13, 14). The two preural segments (corresponding to preural centra 1 and 2) are characterized by the presence of well-developed ventral arcocentra

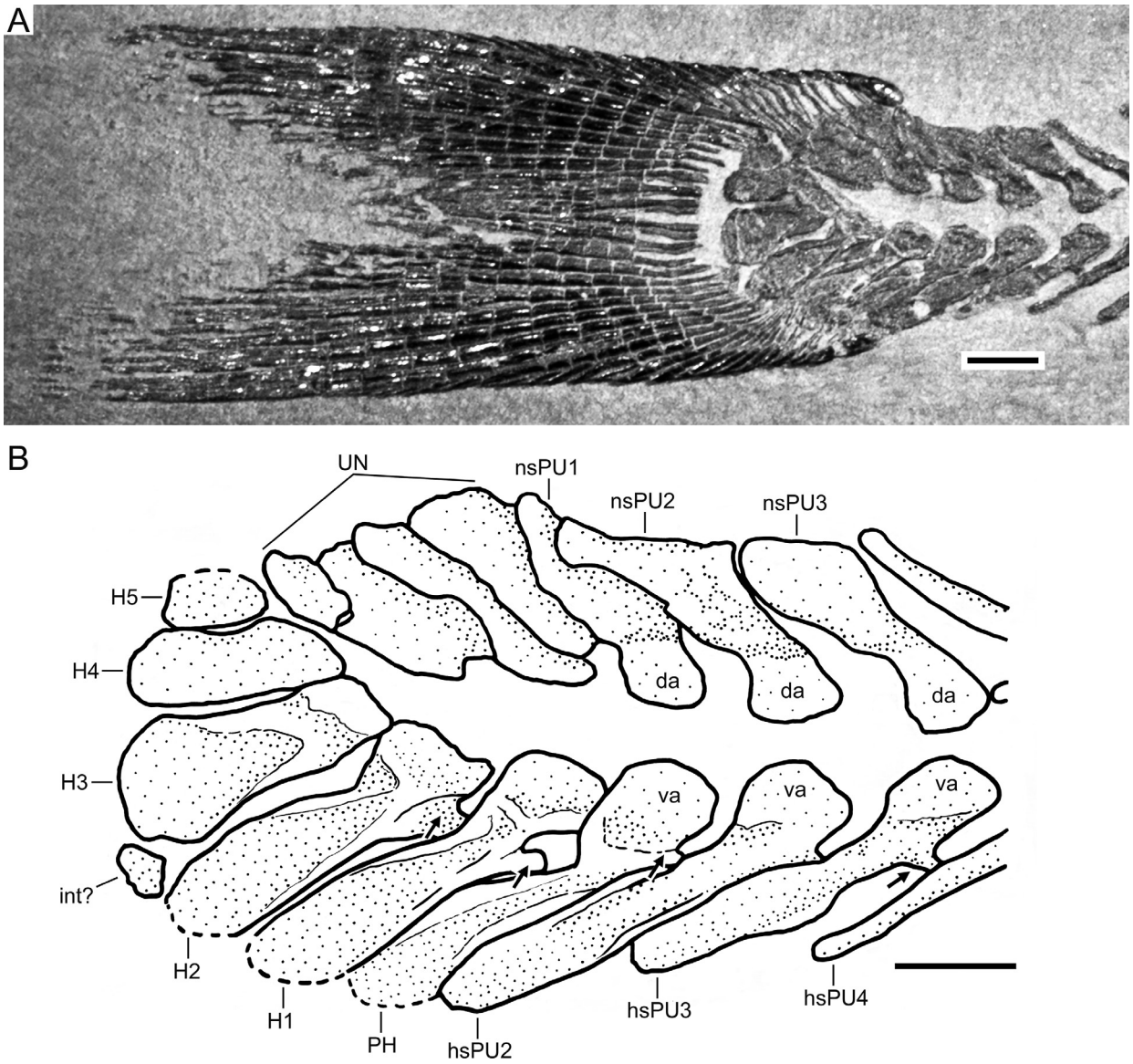

Figure 13. *Marcopoloichthys furreri* sp. nov., illustrating the caudal fin and its endoskeleton. **A.** Photograph of holotype, PIMUZ A/I 2886; photograph was taken by T. Scheyer; **B.** Drawing of endoskeleton. Abbreviations: da, dorsal arcocentra; H1–5, hypurals 1–5; hsPU2–4, haemal spine of preural centra 2–4; int, interhaemal; PH, parhypural ot haemal spine of preural centrum 1; nsPU1–3, neural spine of preural centra 1–3; UN, uroneurals; va, ventral arcocentra. Small arrows point to a series of anterior processes. Scale bars: 1 mm.

with broad and flat haemal spines, which distally support the last principal rays, one procurrent ray, and the series of hypaxial basal fulcra (Figs 13, 14). Dorsally, the neural arches or arcocentra of these two vertebrae are well-developed, and their neural spines are broad and of similar length. The neural spines of the last caudal and preural vertebrae are inclined posteriorly, closer to the body axis, and they do not support the most anterior basal fulcra.

The preservation of the neural spines of preural vertebrae 1–5 suggests they have a central core of cartilage surrounded by a thin, perichondral ossification. In the vertebrae that are completely preserved, an anterior process at the base of neural spines 1–5 is apparently absent. The haemal spines of preural centra 1–3 are moderately broad, but narrower than their respective neural spines. The haemal spine of preural vertebra 4 and more anterior ones are narrower. The haemal spines of the most preural vertebrae are perichondrally ossified thinly. The haemal spines of preural vertebrae 1–3 (Fig. 13) bear a short and narrow anterior process dorsally, at their limit with the expanded ventral arcocentra. A complete neural arch or dorsal arcocentrum, with a well-developed spine, is present on preural centrum 1. A hypurapophysis on the lateral wall of the ventral arcocentrum or haemal arch of preural centrum1 is absent.

Posterior to the neural spine of preural centrum 1, a series of slightly modified chondral neural elements is positioned (Fig. 13). In most specimens, this region is damaged or badly preserved, except for the holotype, which is illustrated in Fig. 13. The first two are elongate laminar elements resembling neural spines, and lacking the ural arcocentra; a third broad, laminar element, also lacking an arcocentrum follows. There is a fourth small, plate-like element posteroventral to the third, which extends caudally between the bases of the epaxial basal fulcra, but it is

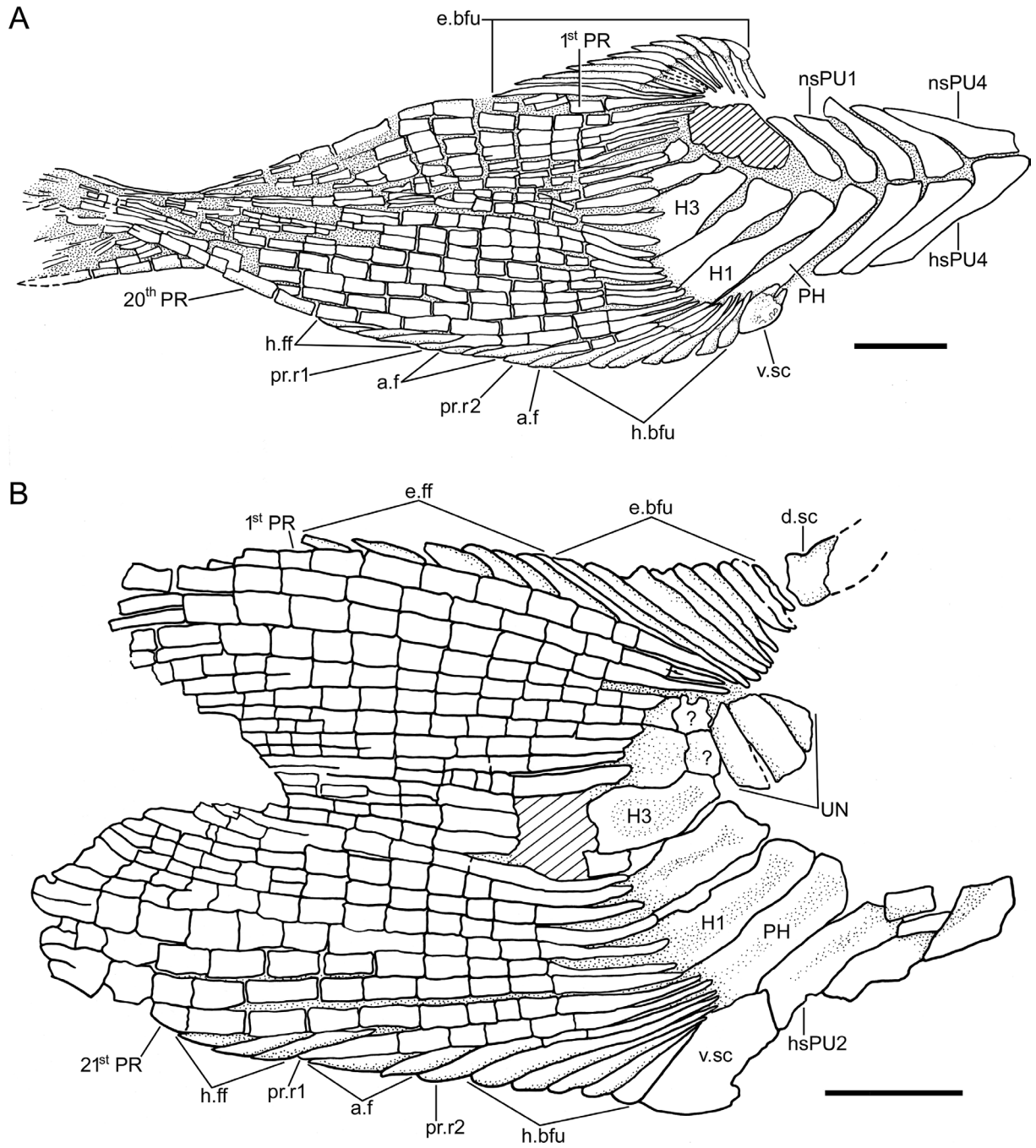

Figure 14. *Marcopoloichthys furreri* sp. nov., illustrating the caudal fin and its endoskeleton. **A.** paratype PIMUZ A/I 2841; area with oblique lines represent a damaged region; **B.** paratype PIMUZ A/I 1958. Abbreviations: a.f, accessory fulcra; d.sc, dorsal caudal scute; e.bfu, epaxial basal fulcra; h.bfu, hypaxial basal fulcra; h.ff, hypaxial fringing fulcra; hsPU4, haemal spine of preural vertebra 4; H1–3, hypurals 1–3; nsPU1, 4, neural spine of preural vertebrae 1, 4; PH, parhypural; pr.r1–2, procurrents rays 1–2; UN, uroneurals; v.sc, ventral caudal scute; 1stPR, first principal caudal ray; 20thPR, principal caudal ray numbered 20; 21stPR, principal caudal ray numbered 21; ?, broken bases of hypurals 4 and 5? Scale bars: 1 mm.

unclear if this could be a broken section of the enlarged third bone. Because of their position as part of the ural region and the lack of their ural neural arches or arcocentra, these bones are considered here as uroneurals "of a special kind". They are different from the uroneural-like elements present in pachycormiforms or some present in aspidorhynchiforms and *Eurycormus*, which are modifications of spines of the preural region. They also differ in shape from the uroneurals of *Leptolepis coryphaenoides* plus more advanced teleosts (see Discussion below). Certainly, these elements in *Marcopoloichthys furreri* sp. nov., because of their position and shape, increase the stiffness of the tail during locomotion, which is a function of the uroneurals.

No epurals are present in the holotype, and there is no space left for them between the distal tips of the enlarged uroneurals and the bases of the epaxial basal fulcra.

Five hypurals (Figs 13, 14) are present, all of them close together so that a diastema between hypurals 2 and

3 is absent. Hypurals 1–4 are slightly expanded at their proximal regions and seem to have preserved part of the ventral arcocentrum. Hypurals 1 and 2 are the longest elements of the series, and hypural 3 is the broadest. A small element is positioned between the distal portions of hypural 2 and 3, and it is interpreted here as an interhemal. Hypural 5 is the smallest of the series of hypurals. Hypurals 1 and 2 (Fig. 13) are weakly supporting the thin bases of part of the hypaxial basal fulcra, the procurrent ray, and the lowest principal rays. Several thin and narrow bases of the principal rays articulate directly with one hypural without producing a special angle.

There are ten or eleven epaxial basal fulcra, which are followed by 10 or 11 fringing fulcra and only reach to the mid-region of the dorsal margin of the first unsegmented principal ray. There are 20 or 21 principal rays that are segmented and branched distally, and their bases are narrow. The articulation between segments of the principal rays is straight. Ventrally, the basal fulcra are usually incompletely preserved so that a total count cannot be given, but the holotype presents 12 hypaxial basal fulcra. There are one or two short procurrent rays that are followed by a short series of hypaxial fringing fulcra; however, PIMUZ A/I 3209 has a third short procurrent ray (Fig. 14). In addition, accessory fulcra are present between the principal rays and the hypaxial basal fulcra (Figs 13, 14). The external surface of the different kind of fulcra and rays is covered by a thin layer of ganoine.

One elongate and slightly oval dorsal scute and a slightly shorter ventral scute (Figs 13, 14) precede the epaxial and hypaxial lobes, respectively. No urodermals have been observed in the available material.

***Scales*.** The body is devoid of scales, with the exception of two to four large oval scales (Figs 2, 3, 10) placed around or close to the urogenital region and a possible elongate one in front of the dorsal fin in one specimen (Fig. 9).

Taxonomic comments

A comparison between the first described marcopoloichthyids from China and Italy (Tintori et al. 2007) and the new species described here is difficult because of the different states of preservation and information provided by the fossil specimens. *Marcopoloichthys ani* from Yunnan Province, S China, is based on four specimens, whereas *M. andreetti* from Lombardy, Italy is based on one complete specimen; *M. faccii* from Fruli, N Italy, is also based on one specimen. Although the holotypes of *M. ani* and *M. andreetti* were described as complete, the illustrations of *M. ani* (the only species illustrated in Tintori et al. 2007) show that several features are poorly preserved. These facts make it difficult for any comparison among them and with *Marcopoloichthys furreri* sp. nov. Although marcopoloichthyids are known from the Middle Triassic, their age differs, with the Chinese *M. ani* being the oldest (Anisian; Tintori et al. 2007), *M. facii* and *M. furreri* sp. nov. lying in the middle (Ladinian; Tintori et al. 2007; present paper, Table 1), and *M. faccii* being the youngest (Early Carnian; Tintori et al. 2007; Dalla Vecchia 2008). Additionally, there are younger (Carnian) specimens reported by Dalla Vecchia (2008) from the middle-late Norian Dolomia di Forni Formation of Friuli Region of NE Italy (Dalla Vecchia 2012, fig. 8.87; pers. comm. May, 2021) that remain undescribed (work in progress together with A. Tintori). Additionally, a possible new species (still undescribed) has been recovered in the Middle Triassic of Monte San Giorgio, Canton Ticino, southern Switzerland (T. Bürgin pers. comm., 2022).

Marcopoloichthys furreri sp. nov. presents the diagnostic characters of the family Marcopoloichthyidae and its only known genus, *Marcopoloichthys*: a naked, torpedo-like body; highly modified protractile upper and lower jaws; vertebral column with persistent notochord and well-developed arcocentral elements; vertebral caudal region diplospondylous, with small interdorsal and interventral elements; ossified ribs absent; large and curved pelvic plates; enlarged, plate-like first dorsal fin proximal radial supporting four or more dorsal rays; enlarged last dorsal proximal radial supporting several dorsal rays; first anal fin proximal radial basally expanded and very elongate; last anal fin proximal radial highly modified into an expanded plate supporting three or more lepidotrichia; no fringing fulcra associated with paired, dorsal, and anal fins; homocercal caudal fin with both lobes deeply forked; body-lobe of caudal fin completely reduced; and a few large scales around urogenital opening.

The new species presents an unreported feature that I have named here supradorsal carrier, which is the result of the fusion of at least the five most anterior abdominal vertebrae in *M. furreri*, with modified expanded hemi-neural spines, and the five expanded anterior supraneurals sit in a median position. I expect that this feature is present in other marcopoloichthyids and diagnostic for the family, a claim that should be checked when better specimens become available.

There are several diagnostic characters supporting *Marcopoloichthys ani* as a new species according to Tintori et al. (2007), but few supporting other species so that the comparison below does not always includes all recognized species. For example, (1) The postparietal and dermopterotic are separate elements in the skull roof of *M. ani*, as illustrated by Tintori et al. (2007: fig. 3), whereas these bones are fused in *M. furreri* sp. nov. (Fig. 5A, B). (2) The anterior articular region of the maxilla is expanded into an oval region in *M. ani*, whereas it is not expanded anteriorly in *M. andreetti*, but is slightly expanded in *M. furreri* sp. nov. (Fig. 5C). The condition is unknown in *M. faccii*. (3) The lower jaw of *M. ani* is "short and deep, with an ascending anterior margin ending with a tip bending downwards" (Tintori et al. 2007: p. 16), and its ventral margin is markedly bent (my interpretation of Tintori et al. 2007: fig. 3A–C). In contrast, the lower jaw in *M. furreri* (Figs 3, 4, 8) has a high dorsal

margin as a result of a well-developed, oval-shaped coronoid process, and its ventral margin is almost straight, with a rounded antero-ventral process. (4) *M. ani* has 37 to 39 vertebral segments, and this means a comparatively longer vertebral column than in *M. furreri* with 33 to 35 vertebral segments. There is no available information for the other species. (5) The last supradorsal bones are positioned between the most anterior proximal dorsal radials in *M. ani*, whereas the last one is placed in front of the large compound first proximal radial in *M. furreri* (Fig. 9). (6) The pectoral fin of *M. ani* has 13 pectoral rays, whereas *M. faccii* has 15 or 16 principal rays; 15 rays seem to be present in *M. furreri*, with the inner ones thinner and shorter than the most lateral ones, a feature not mentioned for the Chinese and Italian species. (7) Eleven pelvic rays are present in *M. ani*, whereas 10 or 11 rays are in *M. furreri*. (8) The first compound proximal dorsal radial in *M. ani* is ax-shaped; it is pear-shaped in *M. andreetti*; it is a massive, compact, rectangular-shaped plate in *M. furreri* that may be formed by the complete or partial fusion of four proximal radials (Fig. 10). (9) The last dorsal proximal radial is boomerang-shaped in *M. ani*, whereas it is regularly arched with the horizontal limb larger than the vertical one in *M. andreetti*. In contrast, the horizontal limb in *M. furreri* is expanded to support several last dorsal rays, and the vertical limb is markedly arched (Fig. 11). (10) The last proximal anal radial has a similar boomerang shape as the last proximal dorsal radial in *M. ani*; whereas it has an elongate and broad distal portion and a thin elongate anterior vertical limb in *M. furreri* (Fig. 11). (11) There are 10 epaxial and seven to 10 hypaxial basal fulcra in *M. ani*, whereas 10 or 11 epaxial basal fulcra and 12 hypaxial basal fulcra are present in *M. furreri*. (12) Eighteen principal rays are present in the caudal fin of *M. ani*; in contrast, 20 or 21 rays are present in *M. furreri*. (13) Three or four hypaxial procurrent rays are present in *M. ani*; in contrast one or two, occasionally three, are present in *M. furreri*. (14) Two urodermals are apparently present in *M. ani*, whereas no urodermals are found in *M. furreri*.

Although the Triassic *Marcopoloichthys* show similarities with another small, scaleless Triassic fish of similar age—*Prohalecites*—major differences separate them, as for example, the dentition presents in *Prohalecites* (Tintori 1990: text-fig. 2) that is lacking in marcopoloichthyids, the round profile of the head with a rostral bone in *Prohalecites* instead of a mesethmoid, one pair of nasal bones instead of two, weak and simple first and last dorsal pterygiophores in *Prohalecites* in contrast to special bony plates resulting from fusion of several proximal dorsal radials in marcopoloichthyids, ossified ribs in *Prohalecites* versus absence in *Marcopoloichthys*, and numerous other differences.

The above list of morphological differences illustrates differences among *Marcopolichthys ani*, *M. andreetti*, and *M. faccii* as described by Tintori et al. (2007) and *Marcopolichthys furreri*, which support *M. furreri* as a new species.

Phylogenetic analysis

First phylogenetic analysis

Two phylogenetic analyses were performed. The first phylogenetic analysis was conducted using a matrix containing numerous neopterygians to test the position of *Marcopoloichthys furreri* sp. nov. within Neopterygii. For this purpose, the matrix of Shen and Arratia (2022) which is a partially modified matrix of Xu (2020a) and contains 55 taxa scored for 137 characters, was used. One character (Ch. 138, absence versus presence of uroneurals) was added. For the details concerning the characters and their coding, see Suppl. material 1, and for the matrix, see Suppl. material 2. *Moythomasia durgaringa*, *Pteronisculus stensioi*, and *Boreosomus piveteaui* represent the outgroup.

The parsimony phylogenetic analysis was performed using PAUP 4.0a169. The topology of the strict consensus is shown in Fig. 15 and is based on 84 most parsimonious trees. The tree length is 382. Consistency index (CI) is 0.4241, and the retention index (RI) is 0.7598. For the description of node support for *Marcopoloichthys furreri* and phylogenetic related taxa, see below and Fig. 15 (Node A, crown-group Neopterygii, and Node B, Teleosteomorpha). An asterisk [*] identifies a character interpreted as uniquely derived.

Nodes 1 and 2, showing unresolved polytomies, represent (Fig. 15) a different topology of the consensus than in Xu (2020a), but the same topology as in Shen and Arratia (2022). Node 1 represents the unresolved polytomies including [*Teffichthys madagascariensis* + *Perleidus altolepis* + [*Plesiofuro mingshuica* + *Meidiichthys browni*] plus [[Louwoichthyiformes + Luganoiiformes + Peltopleuriformes] + [*Venusichthys comptus* + *Habroichthys minimus* + crown Neopterygii]] and is weakly supported by four homoplasies: dermosphenotic does not contact with preopercle (Ch. 36[0]); opercle is nearly equal to, or smaller than, subopercle (Ch. 89[1]); four to six branchiostegal rays present (Ch. 93[2]); and 24 or less principal caudal fin rays (Ch. 111[1]).

Node 2 represents the unresolved polytomy formed by [[Louwoichthyiformes + Luganoiiformes + Peltopleuriformes] + [*Venusichthys comptus* + *Habroichthys minimus* + [crown Neopterygii]] and is weakly supported by two homoplastic characters: ratio of dermopterotic [= or supratemporotabular] or pterotic length to parietal length is less than two (Ch. 12[0]); and teeth only present on the anterior portion of oral margin of maxilla (Ch. 65[1]).

Node A (Holostei plus Teleosteomorpha) is supported by nine synapomorphies, only one being uniquely derived: expanded dorsal lamina in the maxilla lost (Ch. 59[1]*). Eight homoplastic characters also support this node: nasal bones joined in midline (Ch. 8[1]); supraorbital bone present (Ch. 43[1]); supramaxilla present (Ch. 54[1]); and interopercle present (Ch. 83[1]). The following five characters are interpreted as reversals by the parsimony analysis at this phylogenetic level: broad width of posttemporal,

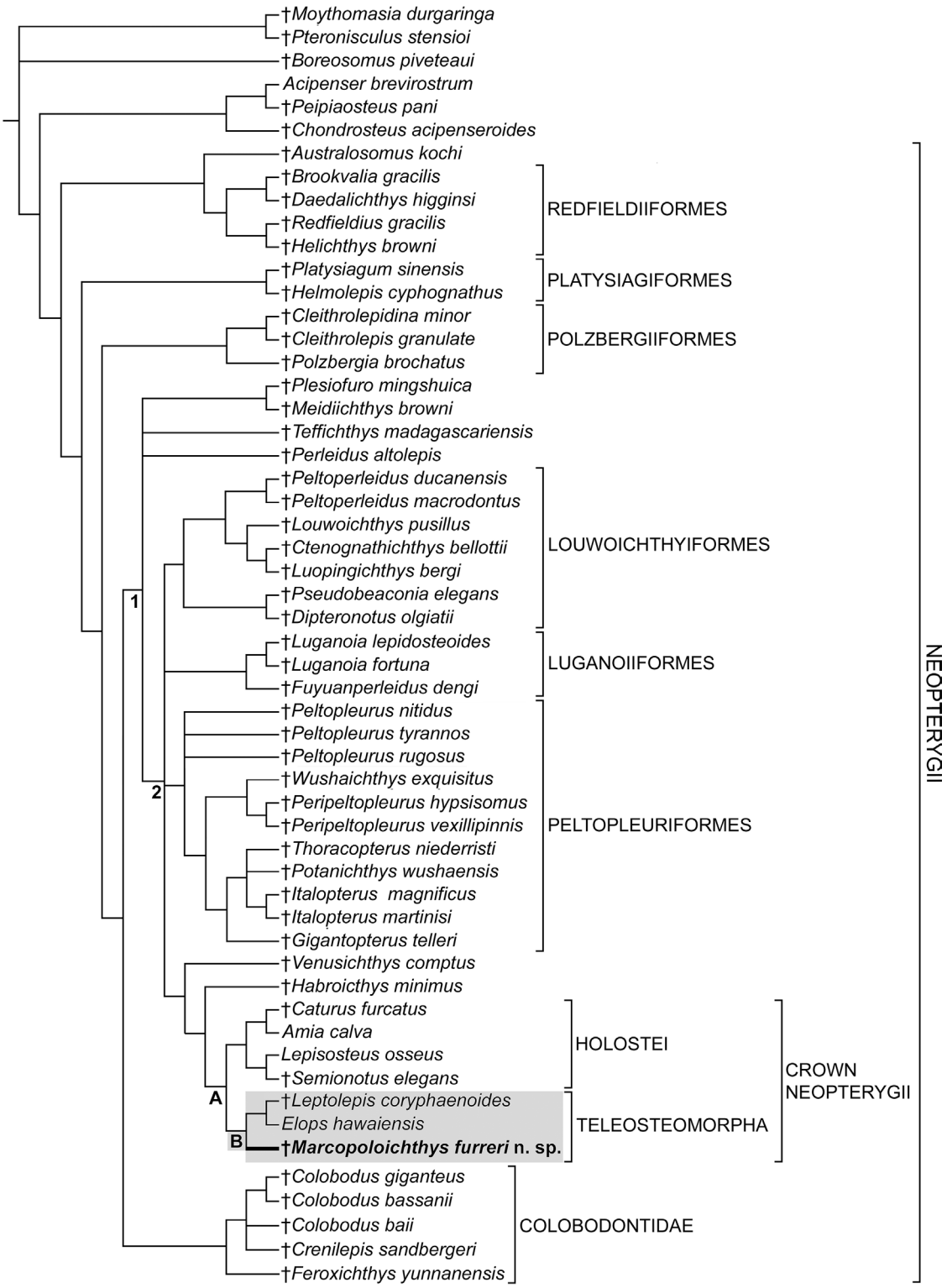

Figure 15. Hypothesis of phylogenetic relationships of *Marcopoloichthys furreri* sp. nov. among neopterygians based on 138 characters and three outgroup taxa. Strict consensus tree of 84 most parsimonious trees: three length 464 steps, consistency index (CI) = 0.3491 and retention index (RI) = 0.6696. An asterisk identifies a uniquely derived character. **Node A** (crown Neopterygii) is supported by the following synapomorphies: supraorbital bone present; supramaxilla present; expanded dorsal lamina in the maxilla lost (*); nasal bones joined in midline; interopercle present; supracleithrum nearly as deep as posterior margin of opercle (Ch. 102[0]); no segmented procurrent rays in dorsal lobe of caudal fin (Ch. 109[0]); and lateral line scales as deep as, or slightly deeper than, those scales above and below (Ch. 124[0]). **Node B** (Teleosteomorpha): supraoccipital present (*); mobile premaxilla present (*); two supramaxillae present (*); vomers fused in adults into a single bone (*); elongated posteroventral process of quadrate present (*); uroneural(s) present (*); cycloid type of scales present (*); and leading margins of the caudal fins formed by the first and last principal rays (*). Homoplasies supporting this node are: basipterygoid process absent; internal carotid foramen on parasphenoid present; single supraorbital bone; suture between opercle and subopercle greatly inclined; origin of dorsal fin slightly posterior or just in front to pelvic fin origin; and fringing fulcra absent on pectoral fins.

nearly as wide as extrascapular (Ch. 100[0]); supracleithrum nearly as deep as posterior margin of opercle (Ch. 102[0]); no segmented procurrent rays in dorsal lobe of caudal fin (Ch. 109[0]); and lateral line scales as deep as or slightly deeper than those scales above and below (Ch. 124[0]). It is interesting to note that according to this analysis, character 8[1], 43[1], and 54[1] are not present in *Marcopoloichthys furreri* and are interpreted by the parsimony analysis as losses. Character 124[0] is not applicable in *M. furreri*, because the fish has a naked body.

Node B (Teleosteomorpha or total group teleosts) is supported by 14 synapomorphies, eight of which are uniquely derived traits: supraoccipital present (19[1]*); mobile premaxilla present (48[1]*); two supramaxillae present (55[1]*); vomers fused in adults into a single bone (72[1]*); elongated posteroventral process of quadrate present (80[1]*); uroneural(s) present (97[1]*); cycloid type of scales present (128[2]*); and leading margins of the caudal fins formed by the first and last principal rays (138[1]*). Homoplasies supporting this node are the following: basipterygoid process absent (Ch. 26[1]); internal carotid foramen on parasphenoid present (Ch. 27[1]); single supraorbital bone (Ch. 44[0]); suture between opercle and subopercle greatly inclined (Ch. 90[1]); origin of dorsal fin slightly posterior or just anterior to pelvic fin origin (Ch. 107[3]); and fringing fulcra absent on pectoral fins (Ch. 120[1]). The condition of characters 19[1], 27[1], and 80[1] is still unknown in *Marcopoloichthys furreri* sp. nov. because of incomplete preservation, and characters 44[0], 55[1], and 128[2] are not applicable to this taxon, because the fish lacks supraorbitals, supramaxillae, and scales and the parsimony analysis interpret them as a synapomorphy of this node that has been lost in *Marcopoloichthys furreri* sp. nov. The parsimony analysis interprets these losses as autapomorphies of *Marcopoloichthys*. *Marcopoloichthys furreri* sp. nov. stands as the sister group of (*Leptolepis coryphaenoides* + *Elops saurus*). Thus, the phylogenetic analysis unambiguously confirms *Marcopoloichthys* as a member of the Teleosteomorpha.

Second phylogenetic analysis

The second phylogenetic analysis was conducted using a matrix containing numerous teleosteomorphs to test the position of *Marcopoloichthys furreri* sp. nov. For this purpose, the matrix of Arratia et al. (2021) which contains 36 taxa scored for 130 characters, was used. Two characters (Ch. 131: absence versus presence of short, stout epineural processes and Ch. 132: presence versus absence of scales on body) were added. For the details concerning the characters and their coding, see Suppl. material 3, and for the matrix, see Suppl. material 4. *Australosomus*, *Birgeria*, and *Polypterus* represent the outgroup.

The parsimony phylogenetic analysis was performed using PAUP 4.0a169. The topology of the strict consensus is shown in Fig. 16 and is based on two most parsimonious trees. The tree length is 374. Consistency index (CI) is 0.4599, and the retention index (RI) is 0.7534. For the description of node support for *Marcopoloichthys furreri* and phylogenetic related taxa, see below and Fig. 16 (Node C, Teleosteomorpha). An asterisk [*] identifies a character interpreted as uniquely derived.

The clade Teleosteomorpha (Pachycormiformes plus more advanced teleosteomorphs) is supported by 15 synapomorphies, six of which are interpreted as uniquely derived: Foramen for glossopharyngeal nerve placed in prootic or prootic-exoccipital suture (Ch. 34[1]*); four pectoral proximal radials present (Ch. 93[1]*); olfactory organ with accessory nasal sacs (Ch. 122[1]*); craniotemporal muscle present (Ch. 123[1]*); heart with two arterial valves (in the conus arteriosus) present (Ch. 124[1]*); and muscles at the basal arteria (ventral aorta) absent (Ch. 125[1]*). Seven homoplasies also support this node: pectoral propterygium fused with first pectoral-fin ray (Ch. [94[1]); dorsal or epaxial leading margin of caudal fin with basal fulcra (Ch. 114[1]); and quadratojugal absent (Ch.127[1]). Characters 122, 123, 124, and 125 are interpreted by the parsimony analysis to be present at this phylogenetic level although they are unknown in fossils due to preservation.

Node D represents the trichotomy including *Marcopoloichthys*, Aspidorhynchiformes, and *Prohalecites* plus more advanced teleosteomorphs. This node is weakly supported by two synapomorphies: supramaxillary bone or most posterior supramaxilla dorsal to maxilla (Ch.58[0]) and mid-caudal centra (adults) with diplospondylous centra (Ch. 87[0]). The parsimony analysis interprets the absence of a supramaxilla in *Marcopoloichthys* as an autapomorphy of this fish.

While in one tree Aspidorhynchiformes, *Marcopoloichthys*, and *Prohalecites* plus more advanced teleosts have resolved relationships, in the second tree, *Marcopoloichthys* is interpreted by the parsimony analysis as the sister of Aspidorhynchiformes.

Node E represents the branching of *Prohalecites* plus more advanced teleosteomorphs. This node is supported by five homoplasies: interparietal [= interfrontal] suture absent (Ch. 22[2]); nasal bones separated from each other by parietal bones [= frontals] (Ch. 23[2]); supraorbital canal with branched tubules (Ch. 35[1]); one supramaxillary bone (Ch. 57[1]); and three or four epurals present (Ch.109[1]).

The consensus tree in Fig. 16, Node F (*Atacamichthys* plus more advanced teleosteomorphs) has an identical topology to that in figure 9 in Arratia et al. (2021).

Discussion and conclusions

Marcopoloichthys and Neopterygii

In the original description of the family Marcopoloichthyidae and its genus *Marcopoloichthys* with three species, Tintori et al. (2007) assigned the family to Neopterygii sensu Patterson (1973), but without assigning the new fish to any neopterygian major taxon. The authors specifically stated in the abstract (p. 13) that “Lack of

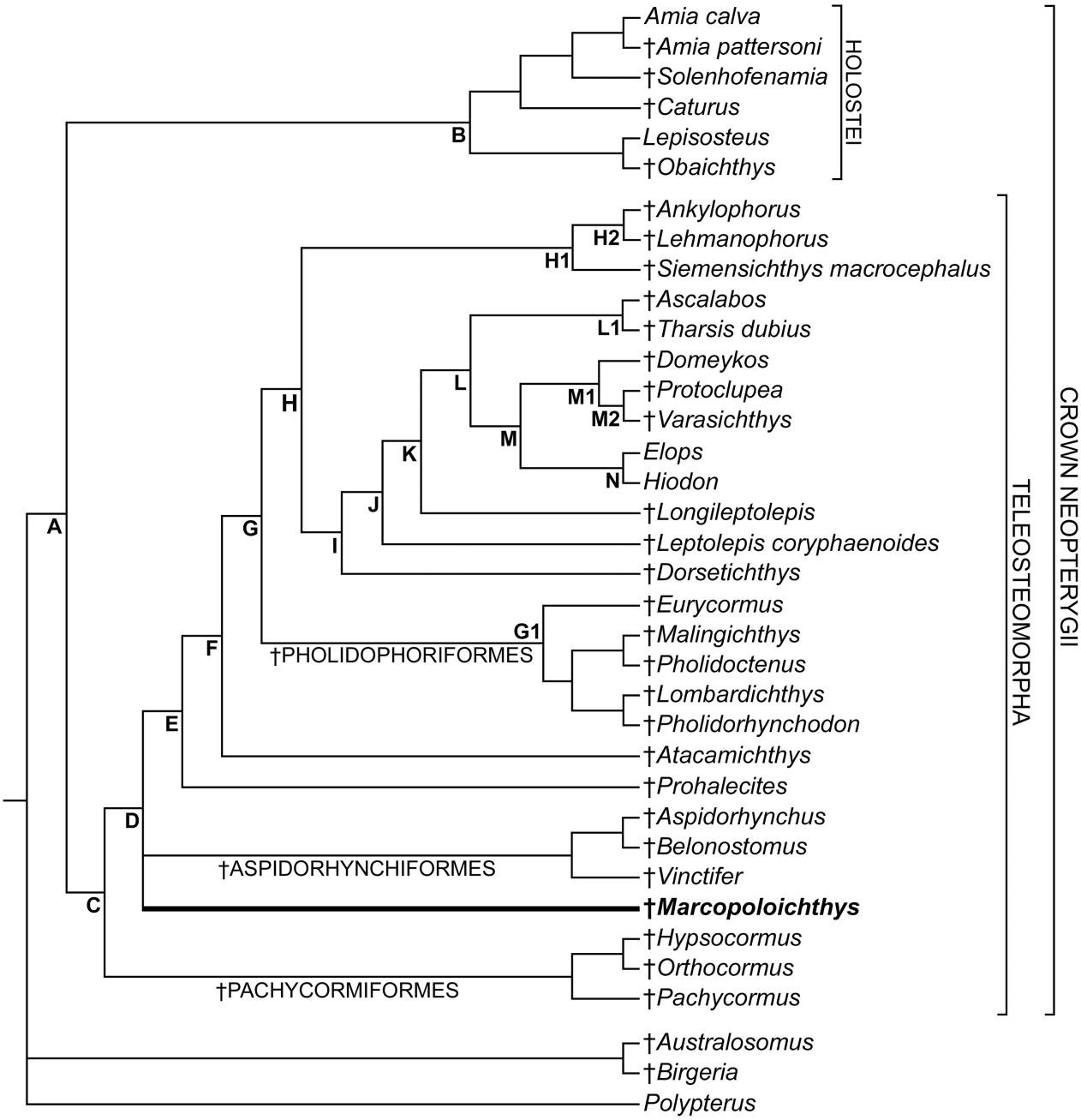

Figure 16. Hypothesis of phylogenetic relationships of *Marcopoloichthys furreri* sp. nov. among crown neopterygians based on 132 characters and three outgroup taxa. Strict consensus tree of two most parsimonious trees: three length 374 steps, consistency index (CI) = 0.4599 and retention index (RI) = 0.7534. An asterisk identifies a uniquely derived character. Teleosteomorphs (**Node C**) are supported by the following synapomorphies: foramen for glossopharyngeal nerve placed in prootic or prootic-exoccipital suture (*); four pectoral proximal radials present (*); olfactory organ with accessory nasal sacs (*); craniotemporal muscle present (*); heart with two arterial valves (in the conus arteriosus) present (]*); muscles at the basal arteria (ventral aorta) absent (*); propterygium fused with first pectoral-fin ray; dorsal or epaxial leading margin of caudal fin with basal fulcra; and quadratojugal absent (Ch.127[1]). **Node D** is supported by two synapomorphies: supramaxilla or most posterior supramaxilla dorsal to maxilla and mid-caudal centra (adults) with diplospondylous centra. For other nodes see text and Arratia et al. (2021).

vertebral centra and epineurals, among others, makes the new taxa quite distinct from true Teleosts, even if some characters may recall the corresponding in Teleosts themselves." Considering their statement and how the understanding of neopterygians has changed, the taxonomic position of *Marcopoloichthys*, as well as its phylogenetic position, were tested based on the new information provided by *Marcopoloichthys furreri* sp. nov. (the best preserved marcopoloichthyid).

Up to 1973, the neopterygians contained the holosteans, but Patterson (1973) proposed a new classification that did not recognize the Holostei as part of the Neopterygii. Later, Grande (2010), based on fossil and living lepisosteiforms, demonstrated the validity of the taxon

Holostei, which has been confirmed in subsequent phylogenetic hypotheses based on morphological (e.g., Arratia 2013; López-Arbarello and Sferco 2018; Xu 2020a, 2020b; 2021; Gouiric-Cavalli and Arratia 2022) and molecular evidence (e.g., Near et al. 2013; Betancur-R. et al. 2013; Betancur-R. et al. 2017). What seems resolved for extant neopterygians has been not so clear for fossil neopterygians with a large and varied record, and whose knowledge has improved during the last years due to new findings, especially in the Triassic of Eurasia (e.g., Xu et al. 2013; Xu and Ma 2016; Xu 2020a, 2020b, 2021).

Although the phylogenetic relationships seem to be resolved for many neopterygian clades, and numerous stem- and crown-group neopterygians are now recognized in recent phylogenetic hypotheses (e.g., López-Arbarello and Sferco 2018; Xu et al. 2015; Xu and Ma 2016; Xu 2020a, 2020b, 2021), the phylogenetic analysis of thoracopteroids by Shen and Arratia (2022), who used the matrix of Xu (2020a), proved to be devastating (see their fig. 3, node 2; Fig. 15 herein) because numerous clades have an unresolved positions within neopterygians. The inclusion of *Marcolopoichthys ferreri* sp. nov. did not change the topology of the consensus (see Fig. 14, node 2) that is similar to that of Shen and Arratia (2022). Nevertheless, we should be aware of the fact that many characters still remain unknown or ambiguous (coded with a question mark) for many of the neopterygians included in the phylogenetic analyses due to incomplete preservation and many nodes are weakly supported so that the phylogenetic position of several taxa still remain controversial and requires further investigation. For instance, Redfieldiiformes (Triassic to Early Jurassic age) have been controversial since the establishment of the family Catopteridae (= Redfieldiidae Berg, 1940) by Woodward in 1890. Discussions on redfieldiiform relationships or phylogenetic analyses including them can be found in Stensiö (1921), Brough (1931, 1936), Schaeffer (1955, 1967, 1984), Hutchinson (1973, 1978), Gardiner and Schaeffer (1989), and more recently in Xu (2021). Redfieldiiformes and Platysiagiformes have been referred as subholosteans, a clade that has not had recognition in fish classification (e.g., Nelson et al. 2016; Arratia 2021). Redfieldiiformes (= family Redfieldiidae) and Platysiagiformes have recently been interpreted as primitive neopterygians by Xu (2020a, 2021; Fig. 15 herein), but as crown actinopterygians, Palaeoniscimorpha, by Schultze et al. (2022).

Finally, the present results suggest marcopoloichthyids as part of the crown-group neopterygians (Fig. 15, node A) and as stem teleosts (Fig. 15, node B), disagreeing with Tintori et al.'s (2007) interpretation that marcopoloichthyids are basal neopterygians.

Marcopoloichthys and Teleosteomorpha

Among Triassic fishes, *Marcopoloichthys* is unique in showing a combination of characters as those in the jaws, endoskeleton of the median fins, or in the reduction of the caudal fin (Tintori et al. 2007). Furthermore, the authors mentioned specifically (p. 13) that "the lack of vertebral centra and epineurals" are characters that question a possible interpretation with "true" teleosts (= *Leptolepis coryphaenoides* plus more advanced teleosts sensu Arratia 1996, 1997, 1999). The presence of a functional notochord or an aspondylous type of vertebral column is true for Ladinian marcopoloichthyids, but a character shared with other teleosteomorphs, such as the Triassic *Prohalecites* (Tintori 1990; Arratia and Tintori 1999) and most pachycormiforms (e.g., Arratia and Schultze 2013; Gouiric-Cavalli 2022). In contrast, other teleosteomorphs, such as Triassic pholidophorids, *Eurycormus* and *Leptolepis coryphaenoides* plus more advanced teleosts, possess vertebral centra formed either by chordacentra or autocentra or both (Arratia 1997, 2013, 2015; Arratia et al. 2001). The statement that marcopoloichthyids lack epineurals is a result of incomplete preservation in the specimens studied by Tintori et al. (2007), but *Marcopoloichthys furreri* sp. nov. has short epineural processes in the abdominal vertebrae and first caudal vertebrae (Figs 3A, 9, 12), and the presence of epineural processes, either short or long, is an undisputed synapomorphy of the apomorphy-based teleosts. Similar short epineural processes are found in another Triassic stem teleost, *Prohalecites*. In addition, *Marcopoloichthys furreri* sp. nov. shares with other teleosteomorphs several undisputed synapomorphies, such as an unpaired vomer (Fig. 4), a mobile premaxilla (Figs 4, 5), lack of prearticular bone in the lower jaw (Fig. 4), four proximal pectoral radials (Fig. 10), propterygium fused with the base of first pectoral ray (Fig. 10), presence of modified ural neural arches or uroneurals (Fig. 13), and first and last principal caudal rays (Fig. 14A) forming the leading margins of the caudal fin (see Patterson 1977 and Arratia 1997, 1999, 2013, 2015 for explanations of these synapomorphies). Because of preservation conditions, it is unknown if other teleostean synapomorphies could be present, such as a supraoccipital bone (Patterson 1975) or a postero-ventral or dorsal process of the quadrate (Arratia and Schultze 1991; Arratia 2013, 2015).

The phylogenetic hypothesis shown in Fig. 15, node B (and descriptions above) confirms *Marcopoloichthys* as a teleosteomorph, phylogenetically closer to *Leptolepis coryphaenoides* and *Elops saurus* than to any other neopterygian clade. The phylogenetic hypothesis shown in Fig. 16, node D confirms *Marcopoloichthys* as a teleosteomorph, with an unresolved phylogenetic position with Aspidorhynchiformes, and [*Prohalecites* plus more advanced teleosteomorphs].

Marcopoloichthys furreri sp. nov. and its complex morphology

Although I refer especially to the new *Marcopoloichthys* from Switzerland, I would expect that some of the morphological characters discussed below are also in other marcopoloichthyids, but due to incomplete preservation

they have not been observed yet. A discussion on selected morphological structures follows.

A strongly ossified T-shaped mesethmoid forming the anterior tip of the snout is an uncommon bone in Triassic and Jurassic teleosteomorphs, which usually have a rostral bone carrying the ethmoidal commissure as in pholidophoriforms (Arratia 2013, 2017) or a special compound rostrodermethmoid as in pachycormiforms (e.g., Lambert 1992; Gouiric-Cavalli and Arratia 2022). The condition in *Marcopoloichthys*, including shape and development of the mesethmoid, resembles that of *Leptolepis coryphaenoides* and *Tharsis dubius* plus more advanced teleosts, such as Elopiformes, Clupeiformes, Ostariophysi, Salmoniformes and many others (Arratia pers. obs.); it differs from them in that the marcopoloichthyid mesethmoid is not sutured with the anterior margin of the parietal [= frontal] bones—it is a free bone.

Marcopoloichthys furreri sp. nov. is remarkable in having two pairs of nasal bones (Figs 4, 5, 6), which are identified here as nasal bones (the anterior pair) that are loosely articulated with the mesethmoid, and an "accessory pair" loosely articulated with the parietal [= frontal] bones posteriorly. The accessory nasal is also a special bone that lies in an almost vertical position in front of the lateral ethmoid when the mouth is closed, and then moving forward in a horizontal position when the mouth is opened (Fig. 7). To my best knowledge, no other teleosteomorph has two pairs of nasal bones; additionally, the bones are unique for the loose articulation between the two pairs and between antimeres, a condition that would permit them to change position during resting and suction feeding. An accessory nasal bone is an autapomorphic feature of *Marcopoloichthys furreri*, and it is expected to be a family character.

An additional structure, named here "rostral cartilage" (Fig. 6), because of its position and structure, is placed below the mesethmoid, probably supporting the latter and offering a smooth surface facilitating the movements of the mesethmoid during feeding.

Marcopoloichthyids lack supramaxillae, in contrast to neopterygians that have one or two supramaxillae on the dorsal margin of the maxilla. In this trait, marcopoloichthyids resemble primitive actinopterygians (Schultze et al. 2022), a feature that becomes a synapomorphy of Marcopoloichthyidae.

The presence of two hypohyals is a common condition in crown teleosts and is also present in such fossils as *Leptolepis coryphaenoides* and more advanced teleosts. The condition remains obscure for several stem teleosts, but among them *Marcopoloichthys furreri* has one hypohyal resembling the condition in holosteans.

A supraneural carrier is a compound structure formed by the fusion of the most anterior neural elements of the vertebral column, bearing five expanded supraneurals (Fig. 9). To the best of my knowledge, this structure is only known in *Marcopoloichthys furreri* but it is expected to be present in other marcopoloichthyids and be a family synapomorphy. See below concerning possible interpretations about the feeding mechanism in *Marcopoloichthys furreri*.

It is interesting that *Marcopoloichthys* specimens show a series of parapophyses in specimens with the abdominal region of the vertebral column well-preserved, but ossified ribs or their remains have not been found in any specimen (Tintori et al. 2007: figs 2, 4; Figs 2, 3, 4, 9 herein). According to the available information, ossified ribs are found in other teleosteomorphs, making this absence a synapomorphy of Marcopoloichthyidae.

Marcopoloichthys furreri sp. nov. possesses three bony postcleithra (Fig. 4) that are mainly positioned in the hypaxial body musculature, forming a series similar to those found in *Leptolepis coryphaenoides*, *Tharsis* and other ascalaboids, and more advanced teleosts, such as crown groups elopiforms, clupeomorphs, many ostariophysans and euteleosts. Certainly, this is a different condition to that found in *Prohalecites* with one bony postcleithrum and neopterygians with modified ganoid scales that are also named postcleithra. Among stem teleosts, the postcleithra of *Marcopoloichthys furreri* appears to be another autapomorphic feature that should be confirmed in other marcopoloichthyids.

The first three or four proximal radials of the dorsal fin fused together forming a broad bony plate that supports the anterior most dorsal fin in marcopoloichthyids is an unquestionable synapomorphy of the group, apparently unique among neopterygians. Additionally, the differences in shape and numbers of radials included in the fusion is of taxonomic value, characterizing some species of marcopoloichthyids. Usually, in teleosteomorphs and crown teleosts, the first dorsal pterygiophore may have one to three processes.

The last dorsal pterygiophore in stem teleosteomorphs and crown teleosts is slightly expanded and supports two dorsal lepidotrichia that are counted as one. The last element in marcopoloichthyids is enlarged and supports more than two lepidotrichia; this is another synapomorphy of the family. The current information concerning the number of lepidotrichia involved is incomplete for all marcopoloichthyid species. A similar situation concerns the last anal pterygiophore, which is also expanded and supports more than two rays, but the total number involved for each species is unclear due to preservation.

Although it is clear that *Marcopoloichthys furreri* represents a new species and that marcopoloichthyids are a well diagnosed taxon, their unique combination of primitive and advanced characters makes it difficult to place them phylogenetically among teleosteomorphs (a study that will be addressed when the youngest marcopoloichthyids from Italy can be added to the study).

Comments on suction feeding mechanism

Studies on the suction mechanism in extant teleosts is a complicated subject that requires a combination of experimental and modeling approaches (e.g., Gibb and Ferry-Graham 2005; Day et al. 2015). It is not my intention to analyze the biomechanics of the feeding suction of *Marcopoloichthys furreri* sp. nov., but the sample of

specimens under study have individuals that died with the mouth closed, whereas others were feeding. It is interesting to analyze the morphological differences between both stages trying to understand, somehow, the positional changes of the bones, the function of additional bones, and the massive ossification of some bones. Because conditions of preservation, soft structures (ligaments, tendons, or muscles) are missing in the fossils.

One of the noteworthy changes that I should mention is the differences in the shape of the head; it is somewhat triangular when the mouth was closed, whereas there is an antero-posterior elongation of the cranium that is accompanied with a dorso-ventral compression during suction (compare Figs 3A and 4; Fig. 7A and 7B), which is often referred to as "functional integration" (Olson and Miller 1951, 1958; Klingenberg 2014). For example, changes in the shape of the upper and lower jaws and expansion of the skull in *Marcopoloichthys* were integrated to generate an intraoral pressure to draw water and prey into the mouth, as has been shown for extant fishes (Lauder 1985; Day et al. 2015; Wainwright et al. 2015). Such action involved multiple integral components: the mesethmoid; nasals; accessory nasals; upper and lower jaws; the whole suspensorium, including the preopercle, and the strong and heavily ossified ceratohyals, which changed position during suction; integration of the cleithrum—strongly expanded antero-ventrally—as well as the clavicle; and support of the pectoral fins by the scapula and coracoid, whose integrated kinetic movements maximized forces and the chance to engulf prey. In this context, I can suggest an explanation for the presence of a previously unreported structure, the supraneural carrier (Fig. 9) in *Marcopoloichthys*. The large head of the fish in comparison to a narrower body with an aspondylous vertebral column (Fig. 4) would need some kind of support for expansion of the cranium during feeding, and it is possible that this was the function of the fused vertebrae forming the supradorsal carrier. A mechanism that in extant teleosts is replaced by an ossified vertebral column, which may include chordacentrum surrounded by autocentrum or autocentrum alone, depending on the taxon.

The integration of these mechanisms in extant teleosts during prey capture also involves lower jaw length and the length of the ascending process of the premaxilla (Kane et al. 2019). Interestingly, the lower jaw of *Marcopoloichthys furreri* has a moderate length and its articular region with the quadrate (and also symplectic in this case) is placed at about the level of the posterior half of the orbit (Fig. 3A), but when the fish was feeding, the lower jaw displaced anteriorly to below the anterior half of the orbit, closer to the anterior orbital margin (Figs 4, 7). *Marcopoloichthys* lacked an ascending process in the premaxilla, which is present with different degrees of development in extant teleosts. The articular regions of the premaxilla and maxilla were weakly developed (Fig. 5A, C), and when the fish was feeding, both bones displaced anteriorly, forming the lateral walls of the buccal tube (Figs 4, 7B). The dorsal part of the buccal tube was formed by a median and strongly ossified mesethmoid (and the rostral cartilage; Fig. 6), which was loosely articulated postero-laterally with the nasals, and which turn were loosely articulated with the accessory nasals and parietal [= frontal] bones posteriorly. I assume that the bones of the snout region and the upper jaw were kept in position by the action of ligaments.

Independent of the evolutionary changes in bone lengths and the presence of specific bones playing a role in the feeding of teleosteomorphs, *Marcopoloichthys furreri* sp. nov. and its exceptional preservation are an outstanding example of the suction feeding mechanism 242–235 million years ago.

Acknowledgements

Special thanks to Heinz Furrer for making specimens of *Marcopoloichthys furreri* sp. nov. available for this study, providing detailed information for each specimen and its collecting data, and valuable assistance with literature on the Prosanto Formation. To Florian Witzmann (Museum für Naturkunde, Berlin, Germany) for assistance with loans of *Marcopoloichthys* specimens. For loan of valuable specimens used in the phylogenetic analyses, I am grateful to H. Bjerring (Stockholm); R. Böttcher and E. Maxwell (Stuttgart); the late C.H. von Daniels (Hannover); H. Jahnke (Göttingen); W. Mette and W. Resch (Innsbruck); G. Viohl, M. Kölbl-Ebert and M. Ebert (Eichstätt); P. Wellnhofer, O. Rauhut, and M. Moser (München); F. Westphal and the late W.-E. Reif (Tübingen); F. Witzmann (Berlin); U. Goehlich (Vienna); A. Paganoni (Bergamo); A. Tintori (Milan); the late C. Patterson and A. Longbottom (London); D. Berman (Cleveland, Ohio); W. Eschmeyer and D. Catania (San Francisco, California); L. Grande, W. Simpson, W. Westneat, and M.A. Rogers (Chicago); A. Simons and V. Hirt (Saint Paul, Minnesota); E. O. Wiley and A. Bentley (Lawrence, Kansas); the late L. Martin and D. Miao (Lawrence, Kansas); the late K. Liem, K. Hartel, the late F. Jenkins, J. Cundiff, and C. Byrd (Cambridge, Massachusetts); J. McEacharan and M. Retzer (Texas); W. Saul (Philadelphia, Pennsylvania); and J.-Y. Zhang (Beijing). Photographs of specimens were kindly taken by Mrs. Carola Radke (Museum für Naturkunde, Berlin, Germany) and by Torsten Scheyer (University of Zurich, Switzerland) as indicated in the respective figures. Flavio Dalla Vecchia (Institut Català de Paleontologia Miquel Crusafont, Spain) helped with photographs on undescribed specimens of *Marcopoloichthys* illustrated in his (2012) book. To Terry Meehan (Lawrence, Kansas, USA) for revision of the style and grammar of the ms. Special thanks to Toni Bürgin (St. Gallen, Switzerland), Giorgio Carnevale (Torino, Italy), and Florian Witzmann (Chief-Editor) for reviewing the manuscript. Many thanks to the private collectors who donated interesting specimens: Alex Dübendorfer (BNM 201166), Christian Obrist (A/I 2888, 2889, 2890) and Elisabeth Schaufelberger (A/I 1923).

References

Arratia G (1997) Basal teleosts and teleostean phylogeny. Palaeo Ichthyologica 7: 5–168.

Arratia G (1999) The monophyly of Teleostei and stem group teleosts. Consensus and disagreements. In: Arratia G, Schultze H-P (Eds) Mesozoic Fishes 2 – Systematics and the Fossil Record. Verlag Dr. Friedrich Pfeil, München, 265–334.

Arratia G (2001) The sister-group of Teleostei: Consensus and disagreements. Journal of Vertebrate Paleontology 21: 767–773. https://doi.org/10.1671/0272-4634(2001)021[0767:TSGOTC]2.0.CO;2

Arratia G (2008) Actinopterygian postcranial skeleton with special reference to the diversity of fin ray elements, and the problem of identifying homologies. In: Arratia G, Schultze H-P, Wilson MVH (Eds) Mesozoic Fishes 4 – Homology and Phylogeny. Verlag. Dr. Friedrich Pfeil, München, 40–101.

Arratia G (2009) Identifying patterns of diversity of the actinopterygian fulcra. Acta Zoologica, Stockholm 90: 220–235. https://doi.org/10.1111/j.1463-6395.2008.00375.x

Arratia G (2013) Morphology, taxonomy, and phylogeny of Triassic pholidophorid fishes (Actinopterygii, Teleostei). Journal of Vertebrate Paleontology, Memoir 13, 33: 1–138. https://doi.org/10.1080/02724634.2013.835642

Arratia G (2015) Complexities of early Teleostei and the evolution of particular morphological structures through time. Copeia 103: 999–1025. https://doi.org/10.1643/CG-14-184

Arratia G (2016) New remarkable Late Jurassic teleosts from southern Germany: Ascalaboidae n. fam., its content, morphology, and phylogenetic relationships. Fossil Record 19(1): 31–59. https://doi.org/10.5194/fr-19-31-2016

Arratia G (2017) New Triassic teleosts (Actinopterygii, Teleosteomorpha) from northern Italy and their phylogenetic relationships among the most basal teleosts. Journal of Vertebrate Paleontology 37(6): e131269. https://doi.org/10.1080/02724634.2017.1312690

Arratia G (2021) Osteichthyes or Bony Fishes. In: Elias S, Alderton D (Eds) Encyclopedia of Geology, 2nd Edn. Elsevier Inc., New York, 121–137. https://doi.org/10.1016/B978-0-12-409548-9.12082-2

Arratia G, Herzog A (2007) A new halecomorph fish from the Middle Triassic of Switzerland and its systematic implications. Journal of Vertebrate Paleontology 27(4): 838–849. https://doi.org/10.1671/0272-4634(2007)27[838:ANHFFT]2.0.CO;2

Arratia G, Schultze H-P (1991) The palatoquadrate and its ossifications: Development and homology within osteichthyans. Journal of Morphology 208: 1–81. https://doi.org/10.1002/jmor.1052080102

Arratia G, Schultze H-P (2013) Outstanding features of a new Late Jurassic pachycormiform fish from the Kimmeridgian of Brunn, Germany and comments on current understanding of pachycormiforms. In: Arratia G, Schultze H-P, Wilson MVH (Eds) Mesozoic Fishes 5 – Global Diversity and Evolution. Verlag Dr. Friedrich Pfeil, München, 87–120.

Arratia G, Schultze H-P, Casciotta J (2001) Vertebral column and associated elements in dipnoans and comparison with other fishes: development and homology. Journal of Morphology 250: 101–172. https://doi.org/10.1002/jmor.1062

Arratia G, Schultze H-P, Gouiric-Cavalli S, Quezada-Romegialli C (2021) The intriguing *Atacamichthys* fish from the Middle Jurassic of Chile – an amiiform or a teleosteomorph? In: Pradel A, Denton J, Janvier P (Eds) Ancient Fishes and their Living Relatives: a tribute to John G. Maisey. Verlag Dr. Friedrich Pfeil, München, 19–36. https://doi.org/10.1080/14772019.2022.2049382

Bellotti C (1857) Descrizione di alcune nuove specie di pesci fossili di Perledo e di alter localita Lombarde. In: Stoppani A (Ed.) Studii Geologici Paleontologici sulla Lombardia. Turati, Milano, 419–438.

Berg LS (1940) Classification of fishes both recent and fossil. Travaux de l'Institut de l'Académie des sciences de l'URSS, 52: 87–517.

Betancur-R R, Broughton RE, Wiley EO, Carpenter K, Lopez JA, Li C, Holcroft NI, Arcila D, Sanciangco M, Cureton JC, Zhang F, Buser T, Campbell MA, Ballesteros JA, Roa-Varon A, Willis S, Borden WC, Rowley T, Reneau PC, Hough DJ, Lu G, Grande T, Arratia G, Orti G (2013) The tree of life and new classification of bony fishes. PLoS Currents 5. https://doi.org/10.1371/currents.tol.53ba26640df0ccaee75bb165c8c26288

Betancur-R R, Wiley EO, Arratia G, Acero A, Bailly N, Miya M, Lecointre G, Orti G (2017) Phylogenetic Classification of Bony fishes. BMC Evolutionary Biology 17: e162. https://doi.org/10.1186/s12862-017-0958-3

Brough J (1931) On fossil fishes from the Karoo system and some general considerations on the bony fishes of the Triassic period. Proceedings of the Zoological Society of London 101: 235–296. https://doi.org/10.1111/j.1469-7998.1931.tb06193.x

Brough J (1936) On the evolution of bony fishes during the Triassic period. Biological Review 11: 385–405. https://doi.org/10.1111/j.1469-185X.1936.tb00912.x

Brough J (1939) The Triassic fishes of Besano, Lombardy. British Museum of Natural History, London, 117 pp.

Bürgin T (1990) Der Schuppenpanzer von *Habroichthys minimus*, einem ungewönlichen Strahlenflosser (Actinopterygii: Peltopleuriformes) aus der Mittleren Trias der Südalpen. Neues Jahrbuch für Geologie und Paläontologie, Monatshefte 1990(11): 647–658. https://doi.org/10.1127/njgpm/1990/1990/647

Bürgin T (1992) Basal ray-finned fishes (Osteichthyes; Actinopterygii) from the Middle Triassic of Monte San Giorgio (Canton Tessin, Switzerland). Schweizerische Paläontologische Abhandlungen, 114: 1–164.

Bürgin T (1999) Middle Triassic marine fish faunas from Switzerland. In: Arratia G, Schultze H-P (Eds) Mesozoic Fishes 2 – Systematics and Fossil Record. Verlag Dr. Friedrich Pfeil, München, 481–494.

Bürgin T, Herzog A (2002) Die Gattung *Ctenognathichthys* (Actinopterygii; Perleidiformes) aus der Prosanto-Formation (Ladin, Mitteltrias) Graubündens (Schweiz), mit der Beschreibung einer neuen Art, *C. hattichi* sp. nov. Eclogae Geologicae Helvetiae 95: 461–469.

Bürgin T, Eichenberger U, Furrer H, Tschanz K (1991) Die Prosanto-Formation—eine fischreiche Fossil-Lagerstätte in der Mittel-trias der Silvretta-Decke (Kanton Graubünden, Schweiz). Eclogae geologicae Helvetiae 84(3): 921–990.

Cavin L, Furrer H, Obrist C (2013) New coelacanth material from the Middle Triassic of eastern Switzerland, and comments on the taxic diversity of actinistians. Swiss Journal of Geosciences 106: 101–177. https://doi.org/10.1007/s00015-013-0143-7

Cavin L, Mennecart B, Obrist C, Costeur L, Furrer H (2017) Heterochronic evolution explains unusual body shape in a Triassic coelacanth from Switzerland. Scientific Reports 7: e13695. https://doi.org/10.1038/s41598-017-13796-0

Cope ED (1887) Zittel's Manual of Paleontology. American Naturalist 17: 1014–1019.

Dalla Vecchia FM (2008) Vertebrati Fossili del Friuli – 450 milioni di anni di evoluzione. Edizione del Museo Friulano di Storia Naturale, Udine, 303 pp.

Dalla Vecchia FM (2012) Friuli 215 milioni di anni fa – Gli straordinari fossili di Preone finestra su di un mondo scomparso. Municipality of Preone, 224 pp.

Day SW, Higham TE, Holzman R, Van Wassenbergh S (2015) Morphology, kinematics, and dynamics: the mechanics of suction feeding in fishes. Integrative and Comparative Biology 55: 21–35. https://doi.org/10.1093/icb/icv032

Egerton MG (1872) Figures and descriptions of British organic remains. Memoirs of the Geological Survey of the United Kingdom 1872(13): 5–35.

Eichenberger U (1986) Die Mitteltrias der Silvretta-Decke (Ducankette und Landwassertal, Ostalpin). Mitteilungen aus den Geologischen Institut der Eidgenössischen Technischen Hochschule und der Universität Zürich, Neue Folge 252, 196 pp.

Furrer H (1995) The Prosanto Formation, a marine Middle Triassic Fossil Lagerstätte near Davos (Canton Graubünden, Eastern Swiss Alps). Eclogae geologicae Helvetiae 88(3): 681–683.

Furrer H (1999) New excavations in marine Middle Triassic Fossil Lagerstätte at Monte San Giorgio (Canton Ticino, Southern Switzerland) and the Ducan Mountains near Davos (Canton Graubünden, Eastern Switzerland). Rivista Museo Civico di Scienze Naturali "Enrico Caffi" 20: 85–88.

Furrer H (2004) So kam der Fisch auf den Berg—Eine Broschüre zur Sonderausstellung über die Fossilfunde am Ducan. Bündner Natur-Museum Chur und Paläontologisches Institut und Museum der Universität Zürich, 32 pp.

Furrer H (2019) Fische und Saurier aus dem Hochgebirge. Fossilien aus der mittleren Trias bei Davos. Neujahrsblatt der Naturforschenden Gesellschaft in Zürich NGZH221, 112 pp.

Furrer H, Froitzheim U, Wurster D (1992) Geologie, Stratigraphie und Fossilien der Ducankette und des Landwassergebiets (Silvretta-Decke, Ostalpin). Eclogae geologicae Helvetiae 85(1): 245–256.

Gardiner BG, Schaeffer B (1989) Interrelationships of lower actinopterygian fishes. Zoological Journal of the Linnean Society 97: 135–187. https://doi.org/10.1111/j.1096-3642.1989.tb00550.x

Gibb A, Ferry-Graham L (2005) Cranial movements during suction feeding in teleost fishes: Are they modified to enhance suction production? Zoology 108: 141–153. https://doi.org/10.1016/j.zool.2005.03.004

Gortani M (1907) *Pholidophorus faccii* nel Raibliano di Cazzaso in Carnia. Rivista Italiana de Paleontologia 13: 117–124.

Gouiric-Cavalli S, Arratia G (2022) A new †Pachycormiformes (Actinopterygii) from the Upper Jurassic of Gondwana sheds light on the evolutionary history of the group. Journal of Systematic Palaeontology 19(21): 1517–1550. https://doi.org/10.1080/14772019.2022.2049382

Grande L (2010) An empirical synthesis pattern study of gars (Lepisosteiformes) and closely related species, based mostly on skeletal anatomy. The resurrection of Holostei. American Society of Ichthyologists and Herpetologists. Special publication 6, Suppl. Copeia 10(2A), [x +] 871 pp. [ISBN: ISSN 0045-8511]

Herzog A (2001) *Peltoperleidus obristi* sp. nov., ein neuer kleiner Strahlenflosser (Actinopterygii, Perleidiformes) aus der Prosanto-Formation (Mitteltrias) von Graubünden (Schweiz). Eclogae Geologicae Helvetiae 94: 495–507.

Herzog A (2003) Die Knochenfische der Prosanto-Formation (Mitteltrias, GR) - Systematik, Funktionsmorphologie und Paläoökologie. PhD Thesis, University of Zürich, Switzerland.

Hutchinson P (1973) A revision of the redfieldiiform and perleidiform fishes from the Triassic of Bekker's Kraal (South Africa) and Brookvale (New South Wales). Bulletin of the British Museum of Natural History (Geology) 22: 235–354.

Hutchinson P (1978) The anatomy and phylogenetic position of *Helychthys*, a redfieldiiform fish from the Triassic of South Africa. Palaeontology 21: 881–891.

Jollie M (1962) Chordate Morphology. Reinhold Publishing Corporation, New York, 478 pp. https://doi.org/10.5962/bhl.title.6408

Kane EA, Cohen HE, Hicks WR, Mahoney ER, Marshall CD (2019) Beyond suction-feeding fishes: Identifying new approaches to performance integration during prey capture in aquatic vertebrates. Integrative and Comparative Biology 59: 456–472. https://doi.org/10.1093/icb/icz094

Klingenberg CP (2014) Studying morphological integration and modularity at multiple levels: concepts and analysis. Philosophical Transactions of the Royal Society B, Biological Sciences 369: e20130249. https://doi.org/10.1098/rstb.2013.0249

Lauder GV (1985) Aquatic feeding in lower vertebrates. In: Hildebrand M, Bramble DM, Liem KF, Wake DB (Eds) Functional Vertebrate Morphology. Harvard University Press, Cambridge, 210–229. https://doi.org/10.4159/harvard.9780674184404.c12

Lambers P (1992) On the ichthyofauna of the Solnhofen Lithographic Limestones (Upper Jurassic), Germany. Unpublished PhD Thesis, University of Gröningen, The Netherlands.

López-Arbarello A, Sferco E (2018) Neopterygian phylogeny; the merger assay. Royal Society Open Science 5: 172337. https://doi.org/10.1098/rsos.172337

Near TJ, Dornburg A, Eytan RI, Keck BP, Smith WL, Kuhn KL, Moore JA, Price SA, Burbrink FT, Friedman M, Wainwright PC (2013) Phylogeny and tempo of diversification in the super radiation of spiny-rayed fishes. Proceedings of the National Academy of Sciences 110(31): 12738–12743. https://doi.org/10.1073/pnas.1304661110

Nelson JS, Grande T, Wilson MVH (2016) Fishes of the World. Fifth edition. J. Wiley & Sons, Hoboken, New Jersey, [XLI +] 707 pp.

Nybelin O (1963) Zur Morphologie und Terminologie des Schwanzskelettes der Actinopterygier. Arkiv for Zoologi 15: 485–516.

Patterson C (1973) Interrelationships of holosteans. In: Greenwood PH, Miles RS, Patterson C (Eds) Interrelationships of Fishes. Zoological Journal of the Linnean Society, London, 233–305.

Patterson C (1975) The braincase of pholidophorid and leptolepid fishes, with a review of the actinopterygian braincase. Philosophical Transactions of the Royal Society of London, Series B, 269: 275–579. https://doi.org/10.1098/rstb.1975.0001

Patterson C (1977) Contributions of paleontology to teleostean phylogeny. In: Hecht MK, Goody PC, Hetch BM (Eds) Major Patterns in Vertebrate Evolution. NATO Advances Study Institute Series, Serie A: 579–643. https://doi.org/10.1007/978-1-4684-8851-7_21

Regan CT (1923) On the skeleton of *Lepidosteus*, with remarks on the origin and evolution of the lower neopterygian fishes. Proceedings of the Zoological Society of London, pt 1–2: 445–461. https://doi.org/10.1111/j.1096-3642.1923.tb02191.x

Rieppel O (1985) Die Trias Fauna der Tessiner Kalpalpen. XXV. Die Gattung *Saurichthys* (Pisces, Actinopterygii) aus der mittleren Trias des Monte San Giorgio, Kanton Tessin. Schweizerische Paläontologische Abhandlungen 108: 1–103.

Schaeffer B (1955) *Mendocinia*, a subholostean fish from the Triassic of Argentina. American Museum Novitates 1737: 1–23.

Schaeffer B (1984) On the relationships of the Triassic and Liassic redfieldiiform fishes. American Museum Novitates 2795: 1–18.

Schaeffer B, McDonald NG (1978) Redfieldiid fishes from the Triassic-Liassic Newark Supergroup of eastern North America. Bulletin of the American Museum of Natural History 159: 129–174.

Schultze H-P (1966) Morphologische und histologische Untersuchungen an den Schuppen mesozoischer Actinopterygier (Übergang von Ganoid- zu Rundschuppen). Neues Jahrbuch für Geologie und Paläontologie, Abhandlungen 126: 232–312.

Schultze H-P (1996) The scales of Mesozoic actinopterygians. In: Arratia G, Viohl G (Eds) Mesozoic Fishes – Systematics and Paleoecology. Verlag Dr. Friedrich Pfeil, München, 83–93.

Schultze H-P (2008) Nomenclature and homologization of cranial bones in actinopterygians. In: Arratia G, Schultze H-P, Wilson MVH (Eds) Mesozoic Fishes 4 –Homology and Phylogeny. Verlag Dr. Friedrich Pfeil, München, 23–48.

Schultze H-P, Arratia G (1988) Reevaluation of the caudal skeleton of some actinopterygian fishes. II. *Hiodon*, *Elops* and *Albula*. Journal of Morphology 195: 257–303. https://doi.org/10.1002/jmor.1051950304

Schultze H-P, Arratia G (1989) The composition of the caudal skeleton of teleosts (Actinopterygii: Osteichthyes). Zoological Journal of the Linnean Society 97: 189–231. https://doi.org/10.1111/j.1096-3642.1989.tb00547.x

Schultze H-P, Arratia G (2013) The caudal skeleton of basal teleosts, its conventions, and some of its major evolutionary novelties in a temporal dimension. In: Arratia G, Schultze H-P, Wilson MVH (Eds) Mesozoic Fishes 5 – Global Diversity and Evolution. Verlag Dr. Friedrich Pfeil, München, 187–246.

Schultze H-P, Mickle KE, Poplin C, Hilton EJ, Grande L (2022) Actinopterygii I. In: Schultze H-P (Ed.) Handbook of Paleoichthyology, vol. 8A. Verlag Dr. Friedrich Pfeil, München, 1–299.

Shen C, Arratia G (2022) Re-description of the sexually dimorphic peltopleuriform fish *Wushaichthys exquisitus* (Middle Triassic, China): taxonomic implications and phylogenetic relationships. Journal of Systematic Palaeontology 19(19): 1317–1342. https://doi.org/10.1080/14772019.2022.2029595

Stensiö E (1921) Triassic fishes from Spitzbergen. Part I. Verlag Holzhausen: Wien, 307 pp. https://doi.org/10.5962/bhl.title.159141

Teng CS, Cavin L, Maxon Jr RE, Sánchez-Villagra MS, Crump JG (2019) Resolving homology in the face of shifting germ layer origins: Lessons from a major skull vault boundary. eLife 8: e52814. https://doi.org/10.7554/eLife.52814

Tintori A (1990) The actinopterygian fish *Prohalecites* from the Triassic of Northern Italy. Palaeontology 33: 155–174.

Tintori A, Sun Z-Y, Lombardo C, Jiang D-Y, Sun Y-L, Rusconi M, Hao W-C (2007) New specialized basal neopterygians (Actinopterygii) from Triassic of the Tethys realm. Geologia Insubrica 10(2): 13–19.

Tintori A, Lombardo C, Jiang D-Y, Sun Z-Y (2011) "*Pholidophorus*" *faccii* Gortani 1907: nuovi dati tassonomici. Gortania 32: 45–52.

Wainwright PC, McGee MD, Longo SJ, Hernandez LP (2015) Origins, innovations, and diversifications of suction feeding in vertebrates. Integrative and Comparative Biology 55: 134–145. https://doi.org/10.1093/icb/icv026

Westoll S (1943) The origin of the tetrapods. Biological Reviews 18: 78–98. https://doi.org/10.1111/j.1469-185X.1943.tb00289.x

Woodward AS (1890) The fossil fishes of the Hawkesbury series of Gosford. Memoirs of the Geological Survey of New South Wales, Paleontology 4: 1–55.

Xu G-H (2020a) *Feroxichthys yunnanensis* gen. et sp. nov. (Colobodontidae, Neopterygii), a large durophagous predator from the Middle Triassic (Anisian) Luoping Biota, eastern YunnaChina. PeerJ 8: e10229. https://doi.org/10.7717/peerj.10229

Xu G-H (2020b) A new stem-neopterygian fish from the Middle Triassic (Anisian) of Yunnan, China, with a reassessment of the relationships of early neopterygian clades. Zoological Journal of the Linnean Society 191: 375–394. https://doi.org/10.1093/zoolinnean/zlaa053

Xu G-H (2021) The oldest species of *Peltoperleidus* (Louwoichthyiformes, Neopterygii) from the Middle Triassic (Anisian) of China, with phylogenetic and biogeographic implications. PeerJ 9: e12225. https://doi.org/10.7717/peerj.12225

Xu G-H, Ma X-Y (2016) A Middle Triassic stem-neopterygian fish from China sheds new light on the peltopleuriform phylogeny and internal fertilization. Science Bulletin 61: 1766–1774. https://doi.org/10.1007/S11434-016-1189-5

Xu G-H, Zhao L-J, Shen C-C (2015) A Middle Triassic thoracopterid from China highlights the evolutionary origin of overwater gliding in early ray-finned fishes. Biology Letters 11: 183–191. https://doi.org/10.1098/rsbl.2014.0960

Supplementary material 1

List of characters and coding used in First Phylogenetic Analysis

Authors: Gloria Arratia
Data type: Characters and their coding (docx. file)
Explanation note: Characters and their coding used in the First Phylogenetic Analysis.

Link: https://doi.org/10.3897/fr.25.85621.suppl1

Supplementary material 2

Matrix used in First Phylogenetic Analysis

Authors: Gloria Arratia
Data type: Matrix, coding of characters (excel file)
Explanation note: Matrix used in the first phylogenetic analysis.

Link: https://doi.org/10.3897/fr.25.85621.suppl2

Supplementary material 3

List of characters and their coding used in Second Phylogenetic Analysis

Authors: Gloria Arratia
Data type: Characters and their coding (docx. file)
Explanation note: List of characters and coding used in the second phylogenetic analysis.

Link: https://doi.org/10.3897/fr.25.85621.suppl3

Supplementary material 4

Matrix with coding of characters used in Second Phylogenetic Analysis

Authors: Gloria Arratia
Data type: Matrix, coding of characters (excel file)
Explanation note: Matrix with coding of characters used in Second Phylogenetic Analysis.

Link: https://doi.org/10.3897/fr.25.85621.suppl4